

1-[[3-Hydroxy-1-adamantyl]amino]acetyl]-2-cyano-(S)-pyrrolidine: A Potent, Selective, and Orally Bioavailable Dipeptidyl Peptidase IV Inhibitor with Antihyperglycemic Properties

Edwin B. Villhauer,^{*,†} John A. Brinkman,[†] Goli B. Naderi,[†] Bryan F. Burkey,[‡] Beth E. Dunning,[‡] Kapa Prasad,[§] Bonnie L. Mangold,^{||} Mary E. Russell,[‡] and Thomas E. Hughes[‡]

Novartis Institute for Biomedical Research, One Health Plaza, East Hanover, New Jersey 07936

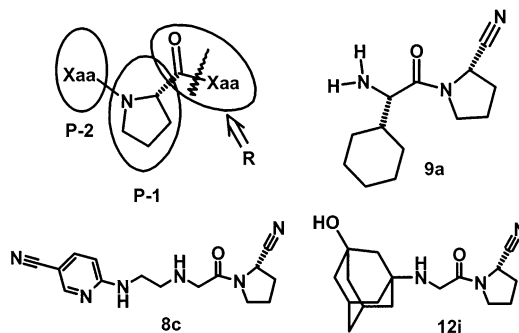
Received February 21, 2003

Dipeptidyl peptidase IV (DPP-IV) inhibition has the potential to become a valuable therapy for type 2 diabetes. The synthesis and structure–activity relationship of a new DPP-IV inhibitor class, N-substituted-glycyl-2-cyanopyrrolidines, are described as well as the path that led from clinical development compound 1-[2-[5-cyanopyridin-2-yl]amino]ethylamino]acetyl-2-cyano-(S)-pyrrolidine (NVP-DPP728, **8c**) to its follow-up, 1-[[3-hydroxy-1-adamantyl] amino]acetyl]-2-cyano-(S)-pyrrolidine (NVP-LAF237, **12j**). The pharmacological profile of **12j** in obese Zucker fa/fa rats along with pharmacokinetic profile comparison of **8c** and **12j** in normal cynomolgus monkeys is discussed. The results suggest that **12j** is a potent, stable, selective DPP-IV inhibitor possessing excellent oral bioavailability and potent antihyperglycemic activity with potential for once-a-day administration.

Introduction

Dipeptidyl peptidase IV (DPP-IV, EC 3.4.14.5) is a ubiquitous yet highly specific serine protease that cleaves N-terminal dipeptides from polypeptides with L-proline or L-alanine at the penultimate position.¹ The biological activities of many circulating regulatory peptides are altered or abolished by the action of DPP-IV in vitro.² However, in part because of the multiplicity of enzymes exhibiting DPP-IV-like activity,³ the in vivo role of DPP-IV in mediating the cleavage of endogenous peptides and the consequences of its inhibition has yet to be established. One exception is with the incretin known as glucagon-like peptide-1 (GLP-1), the most potent insulinotropic hormone known.⁴ Numerous studies with DPP-IV⁵ and DPP-IV inhibitors^{6–10} support a principal role of DPP-IV in the inactivation of GLP-1 in vivo. More importantly, the contribution of DPP-IV catalytic activity to blood glucose control through GLP-1 inactivation has recently been confirmed.¹¹ Because of multiple benefits of GLP-1 augmentation, DPP-IV inhibition has been recognized as a mechanistic approach of potential value in the treatment of type 2 diabetes.¹² Extending the duration of action of GLP-1 would stimulate insulin secretion, inhibit glucagon release,¹³ and slow gastric emptying,¹⁴ each a benefit in the control of glucose homeostasis in patients with type 2 diabetes or its predecessor syndromes. DPP-IV inhibition, through the preservation of active GLP-1 levels, has the potential to slow or even prevent the progression of type 2 diabetes by stimulating insulin gene expression and biosynthesis, increasing the expression of the

Chart 1



β -cell's glucose-sensing mechanism and promoting genes involved in the differentiation (neogenesis) of β -cells.¹⁵ GLP-1 may play a role in acutely suppressing appetite in humans,¹⁶ in mediating peripheral glucose uptake,¹⁷ and may confer maximum glucose sensitivity to the hepatoportal glucose sensor.¹⁸ As the glucose lowering effects of GLP-1 are dependent on elevated blood glucose and subside as glucose levels return to normal, the probability of hypoglycemia during treatment with a DPP-IV inhibitor is expected to be very low.¹⁹ With few exceptions,^{20–22} DPP-IV inhibitors resemble the P2–P1 dipeptidyl substrate cleavage product, where the P-1 site contains a proline mimic.^{23,24} A straightforward replacement of the normally cleaved P-1 substrate amide (R in Chart 1) with an electrophile provides both irreversible (R = P(O)(OPh)₂, CONHOCOR') and reversible (R = B(OH)₂, H, CN) inhibitors.²⁵ The nitrile is especially interesting and provides nanomolar inhibition and chemical stability adequate for oral administration (X_{aa}-(2S)-cyanopyrrolidines^{26–28} and X_{aa}-(4R)-cyanothiazolidines²⁹). Cyclohexylglycine-(2S)-cyanopyrrolidine (**9a**) is one of the more potent, selective, and stable representatives of this nitrile class (K_i of 1.4 nM, >1000-fold selectivity over closely related peptidases and $t_{1/2}$ stability of > 48 h at pH 7.4).²⁷

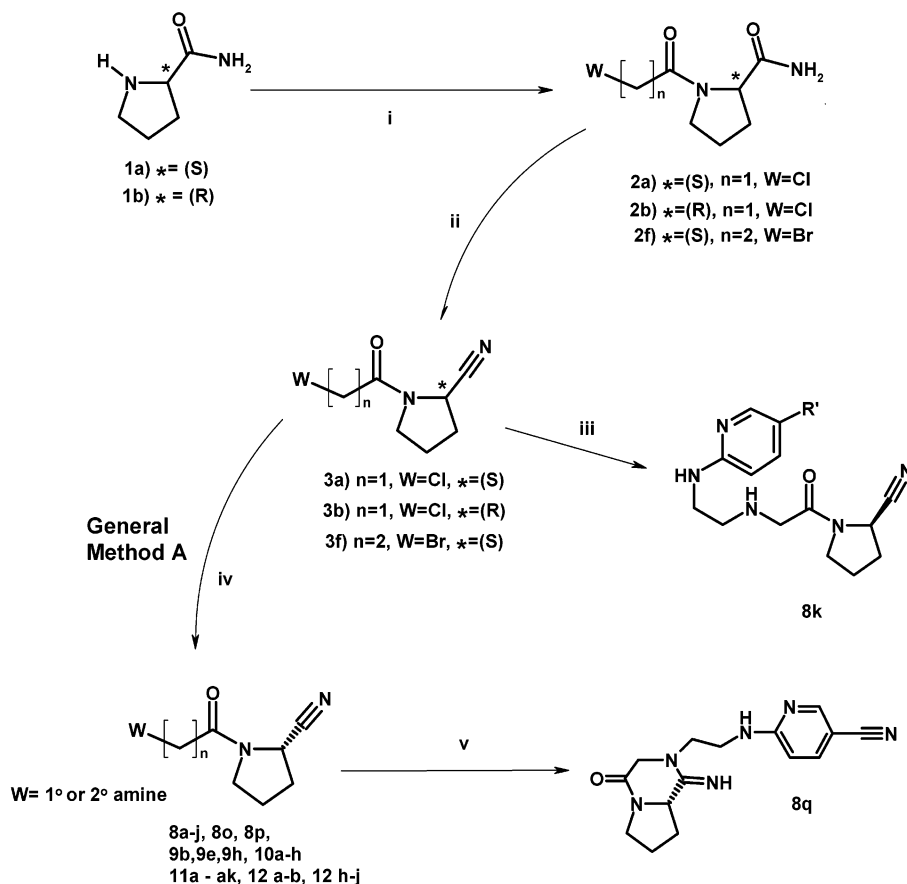
* To whom correspondence should be addressed. Phone: 862-778-8481. Fax 973-781-2188. E-mail: edwin.villhauer@pharma.novartis.com.

[†] Chemistry Department, Metabolic and Cardiovascular Diseases Research.

[‡] Metabolic Diseases Pharmacology Department, Metabolic and Cardiovascular Diseases Research.

[§] Chemical Development.

^{||} Drug Metabolism & Pharmacokinetics Department.

Scheme 1^a

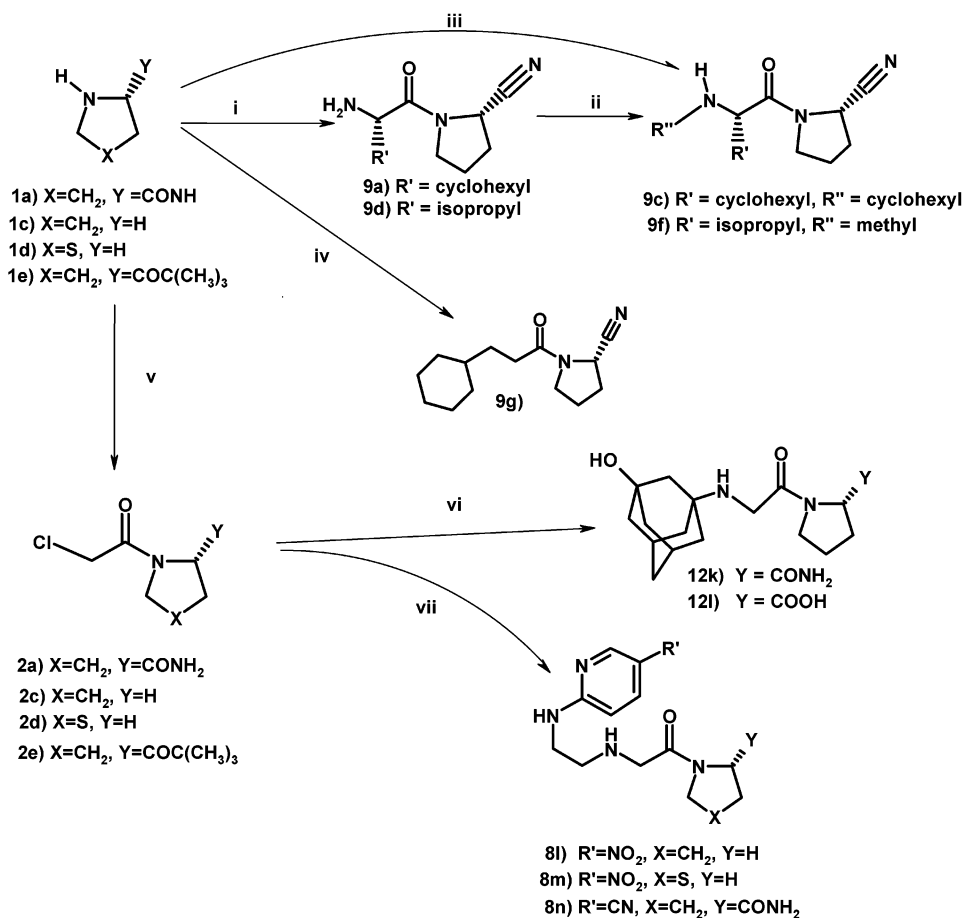
^a Reagents: (i) **1a** → **2a** and **2f**, **1b** → **2b** respectively, ClCH_2COCl for **2a** and **2b**, and $\text{BrCH}_2\text{CH}_2\text{COCl}$ for **2f**, THF or CH_2Cl_2 , base, RT, 18 h; (ii) **2a**, **2b**, and **2f** for **3a**, **3b**, and **3f** respectively, TFAA, THF or CH_2Cl_2 , RT; (iii) **3b**, 2-(2-aminoethylamino)-5-cyanopyridine, K_2CO_3 , THF, RT; (iv) **3a** or **3f** (**3f** only for **8p**), THF, K_2CO_3 , various amines, RT; then TFA/ CH_2Cl_2 only for **11q**; (v) **8c**, 0.5 equiv of tributylamine, EtOAc, reflux, 96 h.

Until recently, a constant in DPP-IV inhibitor design had been an L-amino acid with a protonatable, N-terminal primary amine in the P-2 site (i.e., **9a**). The observation that substrates containing N-methylglycine in the P-2 site were cleaved²³ raised the possibility that structurally more complicated N-substituted glycines may be tolerated at the P-2 site. Through the previous use of a tandem resin-solution parallel synthesis,³⁰ a number of diverse P-2 site N-substituted glycines were prepared and found to provide potent inhibition when combined with a (2S)-cyanopyrrolidide in the P-1 site.^{31–33} Herein is described the structure activity relationship of this class of DPP-IV inhibitors which has led to the selection of slow binding inhibitors NVP-DPP728 (**8c**) and NVP-LAF237 (**12j**) (Chart 1) as clinical development candidates for type 2 diabetes. In addition, a solution-based method for multigram synthesis of this P-2 site N-substituted glycine DPP-IV inhibitor class is described as well as the pharmacological profile of a selective DPP-IV inhibitor, **12j**, which exhibits excellent potency and oral bioavailability.

Chemistry

Pyrrolidine and thiazolidine analogues **8a–q**, **9a–h**, **10a–h**, **11a–ak**, and **12a,b,h–l** were prepared as described in Schemes 1 and 2 and listed in Tables 1–3. As shown in Scheme 1, the addition of chloroacetyl chloride to **1a** and **1b** led to **2a** and **2b**, respectively,

while the addition of 3-bromopropionyl chloride to **1a** led to **2f**. Dehydration of amides **2a**, **2b**, and **2f** with trifluoroacetic anhydride (TFAA) provided nitriles **3a**, **3b**, and **3f**, respectively, which were then coupled with various amines to provide the desired 2-cyanopyrrolidides **8a–k**, **8o**, **8p**, **9b**, **9e**, **9h**, **10a–h**, **11a–ak**, **12 a–b**, **12 h–j** either as the free base, monohydrochloride, dihydrochloride, or TFA salt. Amines used were either commercially available or were known and prepared from literature. These 2-cyanopyrrolidides are stable for months to years if kept as dry solids but will convert to the cyclic amidine with $t_{1/2}$ between 48 h to >70 days in buffered aqueous medium (pH 7.4). They appear as mixtures of cis and trans amide rotomers in solution according to NMR. Compounds **8c** and **12j** are trans amide rotomers in crystalline form as evidenced by the X-ray crystallographic analysis,³⁴ possessing a solubility of >100 mg/mL in distilled water. With minor modifications, the solution synthesis (general method A in Scheme 1) has provided **8c** and **12j** on the 100-kg scale. Intramolecular cyclization of **8c** with 0.5 equiv of tributylamine produced cyclic amidine **8q** after refluxing in EtOAc for 96 h. As shown in Scheme 2, the conversion of **1a** to nitriles **9a**, **9d**, and **9g** was carried out through DIC coupling with N-t-boc-L- α -cyclohexylglycine, N-t-boc-L-valine, N-t-boc-3-methyl-2-methylaminobutyric acid, and cyclohexanepropionic acid, respectively, followed by amide dehydration using POCl_3 for

Scheme 2^a

^a Reagents: (i) **1a**, BocHNCHR'COOH, HOBt, CH₂Cl₂, NMM, DIC, RT, 18 h; then POCl₃, pyridine, imidazole, -30 °C, 1 h; then HCl(g), Et₂O, RT, 18 h; (ii) **9a** → **9c**, cyclohexanone, NaB(O₂CCH₃)₃H, ClCH₂CH₂Cl, RT, 18 h; (iii) **1a** → **9f**, *N*-*t*-boc-3-methyl-2-methylaminobutyric acid, HOBt, CH₂Cl₂, NMM, DIC, RT, 18 h; then POCl₃, pyridine, imidazole, -30 °C, 1 h; then HCl(g), Et₂O, RT, 18 h; (iv) **1a**, 3-cyclohexanepropionic acid, CH₂Cl₂, DMAP, DIC, RT, 6 h, then TFAA, CH₂Cl₂, 0 °C, 2 h; (v) **1a**, **1c**, **1d**, and **1e** → **2a**, **2c**, **2d**, and **2e** respectively, ClCH₂COCl, THF or CH₂Cl₂, K₂CO₃, base, RT, 18 h; (vi) K₂CO₃, THF or CH₂Cl₂, RT, 3-hydroxy-1-aminoadamantane, **2a** for **12k** and **2e** for **12l**; then TFA, CH₂Cl₂, RT for **12l**; (vii) **2c**, **2d**, and **2a** for **8l**, **8m**, and **8n**, respectively, K₂CO₃, THF, 2-(2-aminoethylamino)-5-nitropyridine for **8l** and **8m** and 2-(2-aminoethylamino)-5-cyanopyridine for **8n**, RT.

9a, **9d**, **9f** or TFAA for **9g**. Coupling of amine **9a** with cyclohexanone and reduction of the resulting imine using sodium triacetoxyborohydride provided amine **9c**. Coupling of **2a** and **2e** with 3-hydroxy-1-aminoadamantane³³ provided **12k** and the *t*-boc ester precursor of **12l**, respectively. Acid-catalyzed removal of the *t*-boc-ester using TFA in CH₂Cl₂ led to **12l**. Coupling of 2-(2-aminoethylamino)-5-nitropyridine with **2c** and **2d** provided **8l** and **8m**, respectively, while coupling of 2-(2-aminoethylamino)-5-cyanopyridine with **2f** provides **8n**.

Adamantyl analogues **12c–g** and **12m–r** were prepared as described in Scheme 3 and are listed in Table 3. The *N*-substituted glycine ester **4**, prepared by coupling 1-adamantaneamine and ethyl bromoacetate, was reacted with benzyl chloroformate followed by ester hydrolysis with LiOH to provide glycine derivative **5**. The free acid in **5** was DIC-coupled with various amines followed by CBZ-deprotection via palladium-catalyzed hydrogenation to provide *N*-adamantyl glycine amide derivatives **12c–g**. The hydroxyl group in carbamate **6**³³ was coupled with isocyanates or carbamoyl chlorides to provide bis-carbamates **7a–e** while coupling **6** with acetyl chloride provided ester **7f**. CBZ-deprotection of **7a–e** via palladium-catalyzed hydrogenation followed

by coupling of the resulting adamantylamines with **3a** provided **12m–r**, respectively.

Results and Discussion

The pyrrolidide, thiazolidide, and *N*-substituted glycine amide derivatives described above were tested for inhibition of DPP-IV derived from human colonic carcinoma cells (Caco-2),³⁵ and the results are included in Tables 1–3. An earlier manuscript³⁰ described the solid-phase synthesis of a library of ~200 *N*-substituted glycine-2-cyano-(*S*)-pyrrolidides which provided **8a** as one of a few low nanomolar DPP-IV inhibitors. Starting with **8a**, a focused structure activity profiling effort was initiated by first introducing changes to the P-2 site amine, 2-(2-aminoethylamino)-5-nitropyridine. Replacement of the *p*-nitro group of **8a** with electrophilic groups, such as chloride (**8b**), cyano (**8c**), and trifluoromethyl (**8e**), provided modest decreases in inhibitory potency (4-, 3-, and 10-fold, respectively) while the *o*-trifluoromethyl analogue **8f** significantly reduced potency (>100-fold reduction). Electron-withdrawing group substitutions on the 2-aminopyridine ring do not appear to be essential since only a 4-fold reduction in inhibitory potency relative to the *p*-nitro analogue **8a** is obtained with the *p*-hydrogen substitute (**8g**, IC₅₀ = 33 nM).

Table 1. DPP-IV Inhibitor Data for Templates 8–10^a

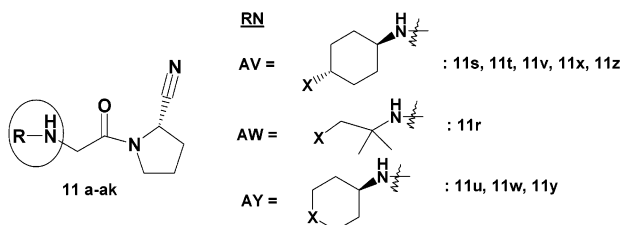
compd	R	U	V	W	X	Y	Z	*	DPP-IV ^b
8a	NO ₂	NH	CN	CH	CH ₂	N	1	S	8 ± 3
8b	Cl	NH	CN	CH	CH ₂	N	1	S	36 ± 5
8c	CN	NH	CN	CH	CH ₂	N	1	S	22 ± 4
8d	H	NH	CN	N	CH ₂	N	1	S	163 ± 39
8e	CF ₃	NH	CN	CH	CH ₂	N	1	S	83 ± 4
8f	H	NH	CN	CCF ₃	CH ₂	N	1	S	989 ± 218
8g	H	NH	CN	CH	CH ₂	N	1	S	33 ± 4
8h	H	NH	CN	CH	CH ₂	CH	1	S	298 ± 113
8i	H	O	CN	CH	CH ₂	CH	1	S	635 ± 112
8j	H	CH ₂	CN	CH	CH ₂	CH	1	S	491 ± 40
8k	CN	NH	CN	CH	CH ₂	N	1	R	1170 ± 21
8l	NO ₂	NH	H	CH	CH ₂	N	1		7400 ± 1,500
8m	NO ₂	NH	H	CH	S	N	1		3000 ± 600
8n	CN	NH	CONH ₂	CH	CH ₂	N	1	S	434 000 ± 20 000
8o	CN	NCH ₂	CN	CH	CH ₂	N	1	S	102 ± 10
8p	NO ₂	NH	CN	CH	CH ₂	N	2	S	18 700 ± 1600
8q									1540 ± 520
9a		H	H	N	H	c-C ₆ H ₁₁			2 ± 0.5
9b		H	H	N	c-C ₆ H ₁₁	H			64 ± 33
9c		H	H	N	c-C ₆ H ₁₁	c-C ₆ H ₁₁			18 600 ± 3900
9d		H	H	N	H	CH(CH ₃) ₂			2 ± 1
9e		H	H	N	CH(CH ₃) ₂	H			192 ± 112
9f		H	H	N	CH ₃	CH(CH ₃) ₂			9610 ± 3590
9g		H	H	CH	c-C ₆ H ₁₁	H			> 500 000, n = 2
9h		H	CH ₃	N	c-C ₆ H ₁₁	H			103 000 ± 8000
10a						H	1		612 ± 148
10b						H	2		80 ± 27
10c						H	3		54 ± 30
10d						CH ₂ OH	3		26 ± 17
10e						CH ₂ OH	4		104 ± 14
10f						H	5		63 ± 13
10g						H	6		53 ± 32
10h						H	10		338 ± 7

^a Values are IC₅₀ (nM) expressed as the mean ± SD of three independent determinations unless otherwise noted. ^b Primary DPP-IV assay in human Caco-2 cells; procedure described in Experimental Section.

Replacement of the 2-aminopyridine ring in **8g**, with pyrimidine (**8d**), aniline (**8h**), phenyl (**8j**), and phenoxy (**8i**) provided increasingly less potent inhibition (5-, 9-, 15-, and 19-fold, respectively, relative to **8g**). Increasing from the ethyl diamine chain found in **8c** to the propyl diamine analogue **8o** provided a modest (4-fold) decrease in inhibitory potency while a dramatic reduction (2300-fold) was observed when the α -amino acid in **8a** was substituted with a β -amino acid (**8p**).

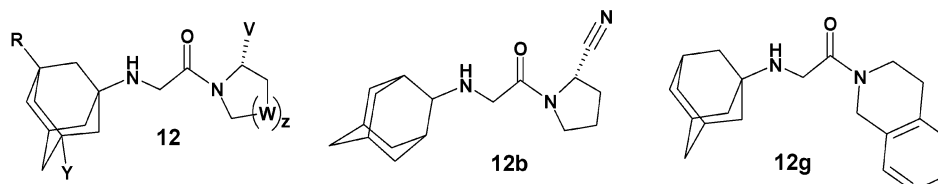
As expected, replacement of the P-1 site 2(*S*)-cyano group in **8c**, which plays a critical role as a transition-state mimetic³⁶ with a 2(*R*)-cyano group (**8k**), significantly reduced potency (53-fold). (Most of the inhibitory potency seen with **8k** can be attributed to ~1% contamination with **8c** which is due to ~1% L-prolinamide contamination in the commercial source of the D-prolinamide starting material. This contamination may also explain the previously reported identical dissociation kinetics between **8c** and **8k** (k_{off} of $1.5 \times 10^{-3} \text{ s}^{-1}$).³⁶) Replacement of the 2(*S*)-cyano group with either a hydrogen (**8l**) or a 2(*S*)-amide (**8n**) dramatically decreased inhibitory potency (900-fold compared to **8a** and 20 000-fold compared to **8c**, respectively). Both des-cyanopyrrolidide (**8l**) and des-cyanothiazolidide (**8m**) provided low μM IC₅₀s, similar to what had been

reported for such P-1 site carbon- and sulfur-containing rings in DPP-IV inhibitor classes possessing amino acid groups in the P-2 site.³⁷ Further evaluation of *p*-cyano analogue (**8c**) in various in vitro DPP-IV and selectivity assays (Table 4) led to its nomination as our first development compound. When compared with the *p*-nitro analogue **8a** and cyclohexylglycine-(2*S*)-cyanopyrrolidide (**9a**),²⁷ **8c** was of comparable activity against human plasma DPP-IV and was significantly more selective for DPP-IV over closely related peptidases, such as post-proline-cleaving enzyme (PPCE) and/or DPP-II.³⁸ Selectivity of **8c** for human plasma DPP-IV over PPCE and DPP-II was 27 000- and 16 000-fold, respectively. In addition, the in vitro specificity of **8c** was profiled in over 100 receptor and enzyme assays, and no significant binding was observed (10 μM). Under neutral and basic aqueous conditions, the P-2 site amine can nucleophilically attack the carbon of the pyrrolidide-nitrile to form the 70-fold less active (attempts to convert **8c** to **8q** resulted in a 1% impurity of **8c**, which may account for most of the observed inhibitory potency seen for **8q**. Attempts to further purify cyclic amidine **8q** via HPLC were not pursued due to facile conversion to the ketopiperazine) cyclic amidine **8q**. Under in vitro assay conditions employed, this intramolecular cycliza-

Table 2. DPP-IV Inhibitor Data for Template 11^a

compd	RN	DPP-IV ^b	compd	RN	DPP-IV ^b
11a	ethylamine	444 ± 35	11p	2-amino-2-methyl-1,3-propanediol	372 ± 92
11b	propylamine	475 ± 45	11q	2-amino-2-methylpropionic acid	10 900 ± 6900
11c	butylamine	261 ± 132	11r to 11z shown below		
11d	pentylamine	266 ± 107	11aa	benzylamine	988 ± 146
11e	hexylamine	282 ± 15	11ab	1-naphthalene-methylamine	436 ± 37
11f	heptylamine	291 ± 12	11ac	phenethylamine	305 ± 51
11g	5-hydroxypentylamine	346 ± 18	11ad	1,1-dimethylphenethylamine	24 ± 5
11h	3,3-dimethylbutylamine	466 ± 18	11ae	3,3-diphenylpropylamine	377 ± 76
11i	1-ethylpropylamine	398 ± 142	11af	2-aminoindane	133 ± 47
11jh	(1 <i>S</i>)-1-(hydroxymethyl)propylamine	256 ± 132	11ag	2-aminobenzimidazole	>1 000 000, <i>n</i> = 2
11k	1-isopropyl-2-methylpropylamine	10 900 ± 5100	11ah	<i>exo</i> -2-aminonorborene	15 ± 8
11l	<i>tert</i> -butylamine	35 ± 7	11ai	(1 <i>R</i> ,2 <i>R</i> ,3 <i>R</i> ,5 <i>S</i>)-(-)-isopinocampheylamine	16 ± 5
11m	1,1-dimethylpropylamine	105 ± 16	11aj	1-adamantanemethylamine	598 ± 204
11n	1,1,3,3-tetramethylbutylamine	123 ± 30	11ak	(-)- <i>cis</i> -myrtanylamine	242 ± 23
11o	2-amino-2-methylpropan-1-ol	218 ± 62			
compd	RN	X for AV, AW, or AY		DPP-IV ^b	
11r	AW	5-cyano-2-aminopyridine		29 ± 2	
11s	AV	5-cyano-2-aminopyridine		5 ± 1	
11t	AV	5-trifluoromethyl-2-aminopyridine		7 ± 0	
11u	AY	5-trifluoromethyl-2-aminopyridine		296 ± 110	
11v	AV	2-aminobenzothiazole		10 ± 1	
11w	AY	2-aminobenzothiazole		228 ± 49	
11x	AV	<i>c</i> -C ₆ H ₁₁ CONH		18 ± 6	
11y	AY	<i>c</i> -C ₆ H ₁₁ CONH		23 ± 6	
11z	AV	<i>p</i> -Cl-C ₆ H ₄ O		14 ± 2	

^a Values are IC₅₀ (nM) expressed as the mean ± SD of three independent determinations. ^b Primary DPP-IV assay in human Caco-2 cells; procedure described in Experimental Section.

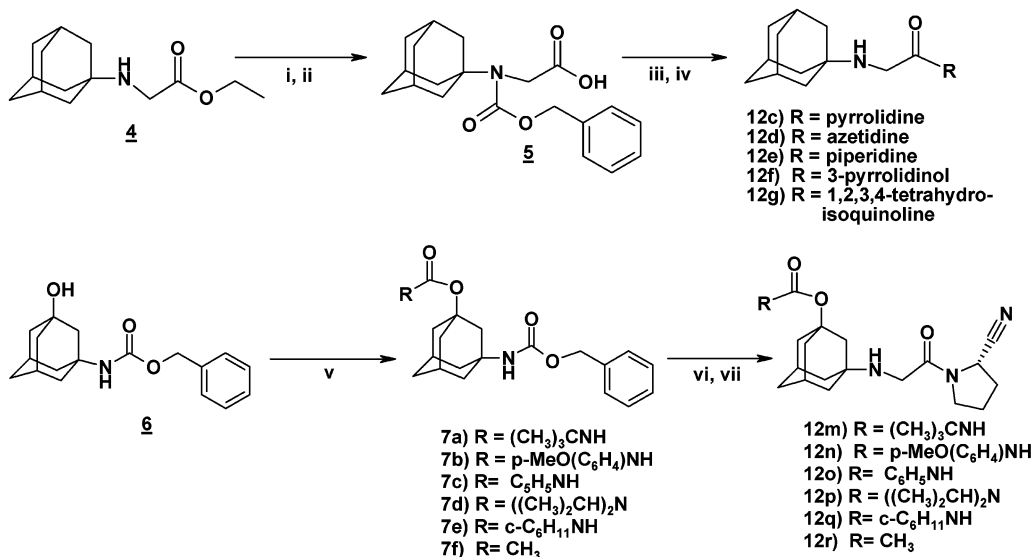
Table 3. DPP-IV Inhibitor Data for Adamantyl Template 12^a

compd	R	Y	V	W	Z	DPP-IV ^b
12a	H	H	CN	CH ₂	1	3 ± 2
12b						13 ± 6
12c	H	H	H	CH ₂	1	7000 ± 1300
12d	H	H	H	CH ₂	0	24 200 ± 5300
12e	H	H	H	CH ₂	2	52 600 ± 8500
12f	H	H	H	CHOH	1	>1 000 000, <i>n</i> = 2
12g						26 100 ± 4900
12h	CH ₂ CH ₃	H	CN	CH ₂	1	7 ± 1
12i	CH ₃	CH ₃	CN	CH ₂	1	17 ± 0
12j	OH	H	CN	CH ₂	1	3.5 ± 1.5
12k	OH	H	CONH ₂	CH ₂	1	931 000 ± 105 000
12l	OH	H	COOH	CH ₂	1	477 000 ± 89 000
12m	OCONHC(CH ₃) ₃	H	CN	CH ₂	1	22 ± 7
12n	OCONH((C ₆ H ₅) <i>p</i> -CH ₃ O)	H	CN	CH ₂	1	149 ± 15
12o	OCONHC ₆ H ₅	H	CN	CH ₂	1	62 ± 5
12p	OCON(CH(CH ₃) ₂) ₂	H	CN	CH ₂	1	183 ± 15
12q	OCONH(<i>c</i> -C ₆ H ₁₁)	H	CN	CH ₂	1	64 ± 16
12r	OCOCH ₃	H	CN	CH ₂	1	70 ± 16

^a Values are IC₅₀ (nM) expressed as the mean ± SD of three independent determinations. ^b Primary DPP-IV assay in human Caco-2 cells; procedure described in Experimental Section.

tion was slow (*t*_{1/2} > 2 days), resulting in less than 1% of **8c** converting during the time frame of the experiments.

According to a recent crystal structure of human DPP-IV complexed with the known inhibitor (valine pyrrolidide),³⁹ the P-2 site valine points into a large cavity

Scheme 3^a

^a Reagents: (i) benzyl chloroformate, CH₂Cl₂, K₂CO₃, RT, 20 h; (ii) LiOH, THF/H₂O, 20 h; (iii) NMM, HOBT, DIC, CH₂Cl₂, various amines; (iv) 10% Pd/C, H₂ (1 atm), EtOAc, RT; (v) **6**, appropriate isocyanate, TMSCl and either CH₂Cl₂, RT, 18 h or ClCH₂CH₂Cl, 50 °C, 18 h for **7a–c,e**; diisopropylcarbonyl chloride for ClCH₂CH₂Cl, 50 °C, 18 h for **7d**; and acetyl chloride, pyridine, DMAP, ClCH₂CH₂Cl, RT, 24 h for **7f**; (vi) 10% Pd/C, H₂ (1 atm), EtOH, RT; (vii) **3a**, THF, K₂CO₃, RT, amines derived from **7a–f** to provide **12m–r**, respectively.

Table 4. DPP-IV Inhibition and Selectivity Assays^a

	Caco-2 ^b	rat plasma ^b	human plasma ^b	PPCE ^c	DPP-II ^d
8a	8.0 ± 3.0	17.3 ± 0.34	8.73 ± 0.79	16 000 ± 1200	12 000 ± 580
8c	22.0 ± 2.0	6.0 ± 1.0	7.0 ± 1.7	190 000 ± 46 000	110 000 ± 5800
9a	2.0 ± 0.3	2.8 ± 0.2	3.15 ± 0.19	41 000 ± 14 000	102 000 ± 20 000
12j	3.5 ± 1.5	2.3 ± 0.1	2.7 ± 0.1	210 000 ± 40 000	>500 000

^a Values are IC₅₀ (nM) expressed as the mean ± SEM of three independent determinations; procedures described in Experimental Section. ^b Primary DPP-IV assays. ^c Extract from human erythrocytes. ^d Extract from bovine kidney homogenate.

in the catalytic binding site and does not make specific contacts with DPP-IV. Due to the importance of the 2(*S*)-cyano group and the use of the P-1 site pyrrolidine ring in our N-substituted glycine series, one can assume that our inhibitors bind DPP-IV in a fashion similar to that observed for valine pyrrolidine. During our SAR effort around **8a**, we explored the steric limitations of DPP-IV's S-2 site cavity first with inhibitors that possess both P-2 site N- and C-substitutions. Whereas proline is a well-known N- and C-substituted cyclic amino acid for the P-2 site in DPP-IV inhibitors,³⁷ little is known about the effect of acyclic N- and C-substituted amino acids. Initial studies suggested that there are significant steric restrictions in this cavity when inhibitors possess both acyclic C- and N-substitutions. Whereas either a C-substituted (**9a**) or N-substituted (**9b**) cyclohexyl group provides low nM inhibition (Table 1), positioning cyclohexyl groups at both the C- and N-terminus (**9c**) significantly reduces potency (9300-fold less compared to **9a** and 290-fold less compared to **9b**). The steric restriction was also observed with significantly smaller lipophilic groups. Whereas a single isopropyl substitution is tolerated on either the P-2 site carbon (**9d**) or nitrogen (**9e**), isopropyl substitution at carbon and methyl at nitrogen (**9f**) was not well tolerated providing significantly reduced potency compared to C-substituted **9d** (4800-fold less). It was found that simple lipophilic and branched C-substitutions provided significantly greater inhibitory effect than N-substitution analogues (**9a/9d** vs **9b/9e**). One can speculate that the N- and C-substitution pattern plays a role in alignment of the basic

terminal amine of inhibitors to form the required salt bridges with DPP-IV's glutamic acids, Glu 205 and Glu 206.³⁹ Inhibitor alignment between DPP-IV's salt bridge formed by Glu 205 and Glu 206, the oxyanion hole, and the S1-pocket may also explain the lack of potency observed with the P-2 site β-amino acid (**8p**) discussed above. As with DPP-IV substrates,^{1,2} a basic, primary, or secondary amine is essential for inhibitory potency as replacement of the N-terminal amine in **9b** with carbon (**9g**) or N-methylation of **9b** to provide a tertiary amine (**9h**) dropped potency by >7800-fold and 1600-fold, respectively.

The study of P-2 site N-substituted glycines continued with the evaluation of various lipophilic ring-sizes (Table 1). The S-2 site pocket of DPP-IV appears to tolerate a large number of lipophilic rings, providing IC₅₀s ranging from 53 nM to 80 nM for four to eight members (**10b**, **10c**, **9b**, **10f**, **10g**) with only a modest drop in potency (5- to 10-fold) for the very small three-membered (**10a**) or rather large 12-membered (**10h**) rings (Table 1). Unlike the simpler ring series where the cyclopentyl (**10c**) and cyclohexyl (**9b**) rings are of similar potency, the hydroxymethylcyclohexyl analogue **10e** is 4-fold less active than the hydroxymethylcyclopentyl analogue **10d**.

As with the above ring systems, inhibitory potency did not vary dramatically (IC₅₀ = 261 to 475 nM, Table 2) between the simple N-terminal linear chain extensions (ethyl to heptyl, **11a–f**), the hydrophilic 5-hydroxypentyl **11g**, or with chain-end sterics found in 3,3-dimethylbutylamine **11h**. As linear chain extensions

were observed to be 4- to 8-fold less potent than ring systems branched near the terminal amine, acyclic chains branching α to the terminal amine were examined further (Table 2). Starting with the simplest branched analogue, isopropyl derivative **9e**, it was found that methylene extensions (1-ethylpropylamine, **11i**) or methylene and hydroxyl extensions (1-hydroxymethylpropylamine, **11j**) only slightly decreased potency. However, steric limits were quickly exceeded with the bis-*gem*-dimethyl extension (**11k**) which provided a 60-fold reduction in potency ($IC_{50} = 10.9 \mu M$) compared to **9e**. Fully branched carbons adjacent to the P-2 site amine proved more interesting as demonstrated with the hydroxymethylcyclopentylamine (**10d**, $IC_{50} = 26 \text{ nM}$) and the *tert*-butylamine groups (**11l**, $IC_{50} = 35 \text{ nM}$). Simple lipophilic and hydrophilic chain extensions on the *tert*-butyl group of **11l** were well tolerated as shown with methyl (**11m**), *tert*-butyl (**11n**), monohydroxyl (**11o**), or bis-hydroxyl (**11p**) groups that only slightly decreased inhibitory potency relative to **11l** (3- to 10-fold). However, replacement of a methyl group from **11l** with a carboxylic acid (**11q**) dramatically reduced potency (300-fold) which may reflect hydrophobic and/or steric limitations.

Cyclic and acyclic branching on the P-2 site pharmacophore of **8c** and **8e** was well tolerated. Substitution of a *gem*-dimethyl group into the 1,2-diaminoethyl chain of **8c** provided the equipotent **11r**, while replacement with a *trans*-1,4-diaminocyclohexyl group provided increased potency as shown with **11s** (4-fold) and **11t** (12-fold), respectively. Substitutions on the *trans*-1,4-diaminocyclohexyl template were well tolerated as shown by the modest potency reductions through replacing the 5-cyano-2-aminopyridine of **11s** with a 2-aminobenzothiazole (**11v**) or a with a cyclohexylamide (**11x**) (2- and 3-fold reduction, respectively). However, replacements with 4-aminopiperidine provided a different profile than observed with the *trans*-1,4-diaminocyclohexyl group. Replacement with 4-aminopiperidine for the 1,2-diaminoethyl chain of **8e** (**11u**) and the *trans*-1,4-diaminocyclohexyl chain in **11t** and **11v** (**11w**) provided >20-fold decreased in inhibitory potency, whereas similar low nM potency was seen for 1,4-diaminocyclohexyl (**11x**) and 4-aminopiperidine (**11y**) analogues containing the cyclohexylamide groups. The advantage of geometrical restriction also carried over into the amino alcohol side chain **11z**, which provided a 45-fold increase in inhibitory potency over the 2-diaminoethane analogue **8i**.

As with the simple aliphatic chains described above, the inhibitory potency of phenyl-substituted aliphatic P-2 site amine extensions, such as benzylamine (**11aa**), 1-naphthalenylmethylamine (**11ab**), phenethylamine (**11ac**), 3-phenylpropylamine (**8j**), and 3,3-diphenylpropylamine (**11ae**), did not vary dramatically ($IC_{50} = 305 \text{ nM}$ to 988 nM , Table 2). Numerous substitutions on benzylamine (**11aa**) and phenethylamine (**11ac**) were explored and showed little effect on potency compared to these unsubstituted analogues (data not shown). Compared to the simpler phenethyl derivative **11ac**, sterics in the form of a *gem*-dimethyl group adjacent to the P-2 site amine (**11ad**) and a conformational constrained ring analogue (**11af**) proved more potent (13- and 2-fold). The fact that the 2-aminobenzimidazole

analogue **11ag** is >7500-fold less potent than the saturated 2-aminoindane analogue **11af** supports the importance of a basic, protonatable P-2 site amine in the N-substituted glycine template for DPP-IV inhibition.

Further explorations of sterics adjacent to the P-2 site amine concentrated on multiple cyclic rings and provided favorable results (Tables 2 and 3). Bicyclic ring systems containing 2-aminonorbornane (**11ah**) and isopinocampheylamine (**11ai**) or tricyclic ring systems containing 1- and 2-adamantylamine (**12a** and **12b**, respectively) all provided very potent inhibitory effect. With an IC_{50} of 3 nM, **12a** was one of the most potent P-2, N-substituted glycine derivatives found. However, lipophilic extensions on **12a** as subtle as the 3-ethyl- (**12h**) and 3,5-dimethyl-1-adamantylamine (**12i**) analogues somewhat reduced inhibitory potency compared to **12a** (2- and 6-fold). The importance of steric ring bulk adjacent to the P-2 site amine is further supported by the dramatic potency decrease seen with methylene insertion between the steric group and the amine in the form of the 1-adamantanemethylamine group in **11aj** and (-)-*cis*-myrtanylamine group in **11ak** (Table 2). With a 1-adamantyl group as the optimal P-2 site substitution, P-1 site requirements were further evaluated starting with the des-cyano analogue of **12a** (**12c**). Although 2300-fold less potent as compared to its 2(*S*)-cyano counterpart, pyrrolidine (**12c**) was noticeably more potent than both azetidine (**12d**) and piperidine (**12e**) P-1 site ring analogues (4- and 8-fold, respectively). As expected, the narrow lipophilic pocket formed by the stacking of Tyr662 and Tyr666 in DPP-IV's catalytic S-1 site³⁹ did not tolerate the hydrophilic nature of the P-1 site 3-pyrrolinol in **12f** which was >330 000-fold less potent than its pyrrolidide counterpart (**12c**). Interestingly, the tetrahydroisoquinoline P-1 site analogue **12g** was as potent as the piperidine P-1 site counterpart **12e**, suggesting either the narrow pocket of DPP-IV's catalytic S-1 site can tolerate a phenyl-extended P-1 site analogue of **12e** or that **12g** binds DPP-IV differently than **12e**.

Examination of primary metabolites of 1- and 2-adamantylamine analogues **12a** and **12b** suggest that monohydroxylation on the adamantyl ring may be well-tolerated in DPP-IV's catalytic S-2 site. To study the effect of monohydroxylation and avoid incorporation of an additional chiral center in monohydroxylation, the 3-hydroxylated-1-aminoadamantane analogue **12j** was prepared. **12j** was noticeably more potent in the Caco-2, rat-, and human plasma DPP-IV assays (6-, 3-, and 3-fold) as well as showing superior efficacy in various in vitro selectivity assays (Table 4) when compared with both **8c** and literature's cyclohexylglycine-(2*S*)-cyano-pyrrolidine (**9a**). **12j** was profiled in over 100 receptor and enzyme assays, and no significant binding was observed ($10 \mu M$). Because of the sterics imposed by the adamantyl group, the ability for **12j** to cyclize to an analogue of imidine **8q** was significantly reduced (>30-fold) compared to that of **8c** and **9a**. To date, **12j** is the most stable DPP-IV inhibitor, possessing a P-1 site transition-state mimetic. The dramatic reduction in inhibitory potency of 2(*S*)-amide (**12k**) and 2(*S*)-acid (**12l**) compared to **12j** (266 000- and 14 000-fold, respectively) provides further support that **12j** binds in the

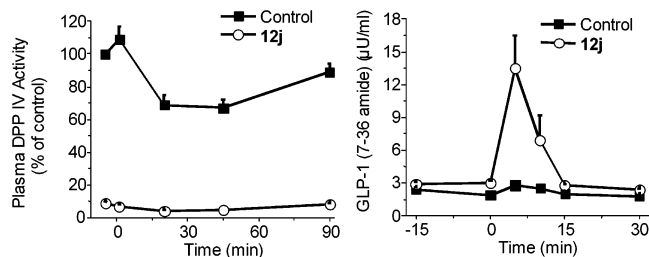


Figure 1. Obese male Zucker rats were orally dosed with CMC or **12j** ($10 \mu\text{mol/kg}$) immediately following the -15 min blood sample collection. Plasma DPP-IV activity (left) and levels of GLP-1 (7–36 amide) (right) were measured during the OGTT. Data were the mean \pm SEM of nine rats/group; procedures are described in Experimental Section. For both DPP-IV activity and GLP-1 (7–36 amide) levels, values for the **12j**-treated rats were significantly different from control at all time points (Student's t -test, $p < 0.05$, except for time -15 min GLP-1 (7–36 amide) levels that were not significant). Plasma DPP-IV activity of -5 min control samples was 3.4 ± 0.9 mU/mL.

S1- and S2-catalytic sites of DPP-IV. Substitutions on the 3-hydroxyl group of **12j** in the form of carbamates (**12m–q**) and ester (**12r**) resulted in significantly reduced potency compared to **12j**. In the carbamate series, potency correlated with size as the diisopropyl analogue **12p** was 8-fold less potent than the *tert*-butyl analogue **12m** while the 4-methoxyphenyl analogue **12n** was 2-fold less potent than both the similarly sized phenyl and cyclohexyl analogues **12o** and **12q**, respectively.

Evaluation of our first development compound (**8c**) in rat,⁹ monkey,³⁰ and human⁴⁰ had previously supported the connection between DPP-IV inhibition and improvement in oral glucose tolerance through an increase in active GLP-1 levels. In a recent chronic study, **8c** was shown to improve glucose tolerance in both normal and glucose-intolerant mice through improved islet function as judged by increased GLUT-2 expression, increased insulin secretion, and protection from increased islet size in insulin resistance.⁴¹ In a continuing effort to explore the pharmacological potential of the N-substituted glycine-2-(*S*)-cyanopyrrolidide class of inhibitor, we evaluated the antidiabetic potential of **12j** in an oral glucose tolerance test (OGTT) with obese Zucker (*fa/fa*) rats which are profoundly insulin-resistant, are markedly glucose intolerant, and represent a rather severe model of Type II diabetes. The results shown in Figure 1 demonstrate that **12j** is a potent, orally active inhibitor of plasma DPP-IV activity that provides increased levels of GLP-1 (7–36 amide). Administration of **12j** ($10 \mu\text{mol/kg}$, po) 15 min prior to a glucose challenge inhibited plasma DPP-IV activity $>90\%$ within 10 min and throughout the 90 min study. The activity in CMC-treated plasma obtained at -5 min was 3.4 ± 0.9 mU/mL and was set as 100%. DPP-IV activity of rats dosed with CMC vehicle declined approximately 35% at 20 and 45 min postglucose challenge. This decline in the control group is attributed to both plasma volume expansion caused by increased osmolarity following the glucose load and to possible plasma dilution caused by frequent blood sampling and donor blood replacement. Prior to **12j** administration (-15 min) plasma levels of GLP-1 (7–36 amide) were no different (CMC vs **12j**; 2.4 ± 0.2 vs 2.9 ± 0.2 pM, (not statistically significant), Student's t -test). However, GLP-1 (7–36 amide) levels were 60% higher ($p < 0.001$,

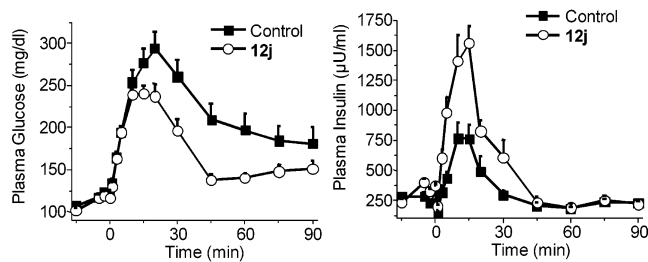


Figure 2. Obese male Zucker rats were orally dosed with CMC or $10 \mu\text{mol/kg}$ **12j** immediately following the -15 min blood sample collection. Glucose was administered orally (1 g/kg) immediately following the time 0 min blood collection. Data were the mean \pm SEM of eight rats/group; procedure is described in Experimental Section. Analysis of the glucose and insulin AUC reveal statistically significant differences between the CMC and **12j** groups.

Student's t -test) in the **12j**-treated rats 15 min after drug administration and before the glucose challenge (0 min). Following the glucose challenge, GLP-1 (7–36 amide) in the drug-treated rats peaked at 5 min at levels that were close to 5 times those of CMC-treated rats (13.5 ± 3.0 vs 2.8 ± 0.2 pM, $p = 0.001$), and returned back to baseline by 15 min. This return to baseline of GLP-1 (7–36 amide) levels by 15 min while DPP-IV is completely inhibited is fully in line with the glucose-dependency of GLP-1 (7–36 amide) secretion from the intestinal L-cell. The results in Figure 2 support the ability of **12j** to both significantly decrease glucose excursions and stimulate insulin secretion. Obese animals receiving CMC were markedly glucose intolerant, with peak glucose levels of 294 ± 19 mg/dL at 20 min while **12j**-treatment decreased the glucose excursion with noticeable differences starting after 5 min and provided peak glucose levels that reached only 241 ± 8 mg/dL at 15 min. Interestingly, while insulin levels were no different between the two groups at the start of the experiment (-15 min), insulin levels were elevated 40% before the glucose challenge in the **12j**-treated group. This modest increase most likely resulted from **12j**-induced preservation of active GLP-1 (7–36 amide) described above. Upon glucose challenge, plasma insulin levels of **12j**-treated rats peaked at levels twice those of vehicle-treated rats and returned to baseline levels by 45 min. The 0 to 45 min insulin AUC was 275% higher in **12j**-treated rats with a corresponding 35% reduction of the 0–45 min glucose AUC. The glucose-stimulated insulin release index (insulin AUC 0–45/glucose AUC 0–45) was ~ 5 -fold greater in the **12j**-treated rats.

The pharmacokinetic profile of **12j** was compared to **8c** in normal cynomolgus monkeys. The absolute oral bioavailability of both **8c** and **12j** were both excellent ($>90\%$) following a $1 \mu\text{mol/kg}$ oral dose while clearance from plasma was moderate ~ 1.3 l/h/kg and ~ 1.5 l/h/kg, respectively. The steady-state volumes of distribution are also moderate for both **8c** (0.8 L/kg) and **12j** (0.7 L/kg), suggesting that both are distributed principally in the body fluids. The C_{max} for **12j** (293 nM at 72 min) is 2.7-fold lower than for **8c** (805 nM at 36 min) while the terminal elimination half-life of **12j** (90 min) is 2.6-fold longer than for **8c** (35 min). Differences seen in the pharmacokinetic profiles of **8c** and **12j** correlated well with observed DPP-IV inhibition pharmacodynamic differences. When comparing the effect on DPP-IV

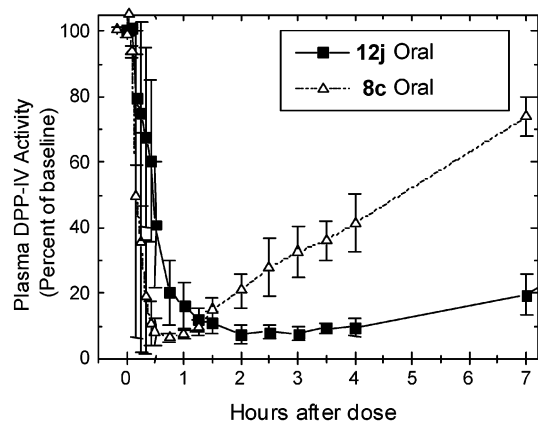


Figure 3. Effects of **12j** (black squares) and **8c** (open triangles) following oral administration of a single $1 \mu\text{mol/kg}$ dose. Values are means \pm SEM of three monkeys **12j** or means \pm range of two monkeys **8c**; procedure is described in Experimental Section.

inhibition in normal Cynomolgus monkeys (Figure 3), maximum inhibition of plasma DPP-IV activity ($\sim 95\%$) was observed approximately 2 h postdose of **12j** ($1 \mu\text{mol/kg}$, po) while $\geq 50\%$ inhibition of DPP-IV was observed within 30 min postdose and persisted for ≥ 10 h (not shown). Maximum inhibition of plasma DPP-IV activity ($\sim 95\%$) occurred within 30 min postdose with **8c** ($1 \mu\text{mol/kg}$, po) but inhibition of $\geq 50\%$ persisted only for 4 to 5 h postdose. As expected with this glucose-dependent mechanism, no hypoglycemia was observed. As a reversible DPP-IV inhibitor with a relatively short half-life, development candidate **8c** might most effectively be taken with a meal when GLP-1 secretion is at maximal rate, while development candidate **12j**, with its longer half-life, provides a better profile for once-a-day treatment if desired. The results of these pharmacological studies suggest that **12j** is a potent, selective, and orally active inhibitor of DPP-IV that improves insulin secretion and glucose homeostasis with a profile wholly consistent with increased action of glucagon-like peptide-1.

Experimental Section

Chemistry. All melting points (mp) were obtained on a Thomas-Hoover capillary melting point apparatus and are uncorrected. Proton NMR (^1H NMR) and carbon NMR (^{13}C NMR) spectra were obtained on a Bruker AC 300-MHz spectrometer. Chemical shifts were recorded in ppm (δ) and were reported relative to the solvent peak or TMS. Chemical shifts recorded for carbon NMR spectra comprised both trans and cis amide rotomers without further delineation. Mass spectra were run on a Finnigan Mat 4600 spectrometer. Elemental analyses, performed by Robertson labs, are within 0.4% of theoretical values. Analytical results were within $\pm 0.4\%$ of the theoretical value. Fractional moles of water and solvent frequently found in some analytical samples were not removed despite 24–48 h of drying in a vacuum and were confirmed, where possible, by their presence in the ^1H NMR spectrum. Optical rotation measurements were performed on a JASCO P-1030 polarimeter, 589 nm, cell length 1 dm, at 20 $^\circ\text{C}$. Column chromatography separations were carried out using Merck silica gel 60 (mesh 230–400) employing a SIMS/Biotage apparatus. Reagents and solvents were purchased from common suppliers and were utilized as received. All reactions were conducted under a nitrogen atmosphere at room temperature with a calcium sulfate drying tube unless noted otherwise. Yields were of purified product and were not optimized. All starting materials and amines were com-

mercially available unless otherwise indicated. Experimentals for **8b**, **8d–j**, **8o**, **9b**, **9e**, **9h**, **10a–h**, **11a–ak**, **12a–b**, and **12h–i** follow General Method A and are found in the Supporting Information.

1-Chloroacetyl-2-(S)-pyrrolidinecarboxamide (2a). A solution of L-prolinamide (**1a**) (5.0 g, 43.9 mmol) in THF (100 mL) was added dropwise over 0.5 h to a stirred mixture of chloroacetyl chloride (3.50 mL, 43.9 mmol) and K_2CO_3 (24.0 g, 175 mmol) in THF (50 mL) at ambient temperature. The reaction mixture was then stirred at room temperature for 18 h and filtered and the filtrate concentrated to provide the desired amide **2a** as a clear, taffy (7.46 g, 89%); ^1H NMR (CDCl_3) 1.94–2.45 (m, 4H), 3.54–3.65 (m, 1H), 3.65–3.75 (m, 1H), 4.08–4.18 (m, 2H), 4.57–4.67 (m, 1H), the two amide hydrogens spread from 6.1 to 7.2 with small broad peaks at 6.18 and 7.04; MS m/z (rel intensity, %) 191 (M^+ , 100), 193 (M^+ , 33).

1-Chloroacetyl-2-cyano-(S)-pyrrolidine (3a). A solution of L-prolinamide (**1a**) (10.0 g, 87.7 mmol) in THF (300 mL) was added dropwise over a period of 0.75 h to a mechanically stirred solution of chloroacetyl chloride (6.99 mL, 87.7 mmol) and K_2CO_3 (48.5 g, 351 mmol) in THF (100 mL). After another 2 h of being stirred, the reaction was filtered to remove potassium salts, and the filtrate was dried over Na_2SO_4 (30 g). This solution of **2a** was again filtered, and to the colorless filtrate was added trifluoroacetic anhydride (19.8 mL, 0.140 mmol) in one portion. The resulting clear, light amber reaction was stirred for 1 h at RT. EtOAc (30 mL) was added prior to rotovap concentration (water bath $<45^\circ\text{C}$) with two more EtOAc chasings ($2\times$) once the concentrate was ~ 25 mL. The resulting clear, light-orange solution was then partitioned between EtOAc and saturated NaHCO_3 , and the aqueous layer was washed twice with EtOAc. The combined organic layers were then successively washed with water and brine, dried over Na_2SO_4 , filtered, and concentrated to obtain 1-chloroacetyl-2-(S)-pyrrolidinenitrile as clear, amber oil. This oil solidified quickly to provide the target product **3a** (7.82 g, 52%) as a yellow-white solid; mp $53\text{--}57^\circ\text{C}$; ^1H NMR (CDCl_3) (4 to 1 mixture of trans/cis amide rotomers): δ 2.10–2.40 (m, 4H), 3.55–3.66 (m, 1H), 3.66–3.79 (m, 1H), 4.03–4.21 (m, 0.4H, CH_2Cl), 4.09 (s, 1.6H, CH_2Cl), 4.76 (m, 0.8H, CHCN), 4.87 (dd, 0.2H, $J = 7.4$ and 2.2 Hz, CHCN); ^{13}C NMR (CDCl_3): δ 165.15, 117.72, 46.95, 46.82, 46.64, 46.37, 41.41, 32.32, 29.81, 25.05, 22.61; MS m/z (rel intensity, %) 173 (M^+ , 100), 175 (M^+ , 33).

General Method A. A 0.5 M solution of **3a**, **3b**, or **3f** (1 equiv) in THF was added dropwise over 0.5 h into an ice-water-cooled 0.3 M mixture of the appropriate amine (2 to 3 equiv) and K_2CO_3 (3 equiv) in THF. The resulting reaction was stirred at ice-water temperature for 2 h and then at room temperature for 1 to 3 days. The resulting mixture was then filtered to remove K_2CO_3 , concentrated, and then partitioned between CH_2Cl_2 and saturated aqueous NaHCO_3 . The aqueous layer was then washed with CH_2Cl_2 ($2\times$), and the combined organic layers were washed with water, dried over Na_2SO_4 , concentrated in vacuo, and chromatographed on silica gel with 5% CH_3OH in CH_2Cl_2 or 20% EtOAc in hexane to provide the free base of the target product. Alternatively, the reaction may be carried out using CH_2Cl_2 as solvent in the reaction while EtOAc may be substituted for CH_2Cl_2 in the partitioning with water. The free base may be converted to the mono- or dihydrochloride salt by slowly passing HCl gas into a 0.1 M solution (THF or Et_2O) of the free base. The resulting solids are then filtered and dried in vacuo. The amine coupling step with **3a** or **3b** provided chromatographed yields that ranged between 30 to 50%.

1-[[[2-[(5-Nitro-2-pyridinyl)-amino]ethyl]amino]acetyl]-2-cyano-(S)-pyrrolidine, Dihydrochloride (8a). Method A: 2-(2-aminoethylamino)-5-nitropyridine³¹ as amine and use of **3a**. Product was a light vanilla-colored solid: mp = 205–208 $^\circ\text{C}$ decomp; ^1H NMR (D_2O) (trans and cis rotomers in a ratio of 9:1): δ 2.01–2.17 (m, 2H), 2.20–2.30 (q, 2H, $J = 5$ Hz), 3.36–3.49 (m, 3H), 3.55–3.64 (m, 1H), 3.82 (t, 2H, $J = 5$ Hz), 4.10 (s, 2H), 4.72 (t, 9/10H, $J = 5$ Hz, HCN), 4.90 (bd, 1/10H,

$J = 7$ Hz, HCN), 6.81 (d, 1H, $J = 9$ Hz), 8.27 (bd, 1H, $J = 9$ Hz), 8.90 (d, 1H, $J = 1$ Hz); (isobutane/DCI) MH/e 318 (MH⁺) of free base; Anal. (C₁₄H₁₈N₆O₃·2HCl·0.2H₂O·0.1THF) C, H, N, Cl.

1-[[[2-[(5-Cyano-2-pyridinyl)amino]ethyl]amino]acetyl]-2-cyano-(S)-pyrrolidine, Dihydrochloride (8c). Method A: 2-(2-aminoethylamino)-5-cyanopyridine³¹ used as amine and use of **3a**. Product was an off-white solid; OR: [d] = -77.152, 12.25 mg/mL in MeOH; white solid; mp: 155–157 °C; ¹H NMR (D₂O) (trans and cis amide rotomers in a ratio of 5:1): δ 2.15–2.30 (m, 2H), 2.35–2.43 (m, 2H), 3.50–3.60 (m, 1H), 3.63–3.75 (m, 1H), 3.80 (t, 2H, $J = 6$ Hz), 3.90 (t, 2H, $J = 6$ Hz), 4.19 (s, 2H), 4.85 (t, 5/6H, $J = 6$ Hz, HCN), 5.00 (dd, 1/6H, $J = 8$ and 1 Hz, HCN), 6.99 (d, 1H, $J = 9$ Hz), 7.97 (dd, 1H, $J = 11$ and 1 Hz), 8.50 (s, 1H). (isobutane/DCI) MH/e 299 (MH⁺) of free base; Anal. (C₁₅H₁₈N₆O·2.0HCl·0.19H₂O·0.30THF) C, H, N.

1-[[[2-[(5-Cyano-2-pyridinyl)amino]ethyl]amino]acetyl]-2-cyano-(S)-pyrrolidine, Dihydrochloride (8k). D-Prolinamide (**1b**) (commercial source contaminated with ~1% L-prolinamide) was converted to 1-chloroacetyl-2-cyano-(R)-pyrrolidine (**3b**) following the procedure of **3a**. The synthesis for dihydrochloride of **8c** was then followed. Product was a white solid; mp = 152–154 °C; ¹H NMR (D₂O) (trans and cis amide rotomers in a ratio of 5:1): δ 2.17–2.27 (m, 2H), 2.35–2.45 (m, 2H), 3.48–3.60 (m, 2H), 3.67–3.75 (m, 1H), 3.79–3.87 (m, 1H), 3.93 (t, 2H, $J = 6$ Hz), 4.22 (s, 2H), 4.87 (t, 5/6H, $J = 6$ Hz, CHCN), 5.00 (dd, 1/6H, $J = 8$ and 2 Hz, CHCN), 7.01 (d, 1H, $J = 9$ Hz), 7.99 (dd, 1H, $J = 10$ and 1 Hz), 8.48 (d, 1H, $J = 1$ Hz); (isobutane/DCI) MH/e 299 (MH⁺) of free base; Anal. (C₁₅H₁₈N₆O₁·1.95HCl·0.50H₂O·0.50THF) C, H, N.

1-[2-(5-Nitropyridin-2-yl)amino]ethylamino]acetylpyrrolidine, Dihydrochloride (8l). A solution of pyrrolidine **1c** (2.50 g, 35.0 mmol), triethylamine (3.90 mL, 38.7 mmol), and 20.0 mg of (dimethylamino)pyridine (DMAP) in CH₂Cl₂ (20.0 mL) was added, dropwise to an ice-cold solution of 3.08 mL (38.7 mmol) of chloroacetyl chloride in 20.0 mL of CH₂Cl₂, over a period of 60 min. The resulting solution was then stirred at ice–water temperature under a calcium sulfate drying tube for 2 h and then at room temperature for 16 h. The solution was poured into 150 mL of EtOAc and the resulting white precipitate filtered. The filtrate was washed with ethyl acetate and concentrated in vacuo to obtain 3.80 g of crude 1-chloroacetylpyrrolidine (**2c**). In a 200 mL flask was dissolved 14.3 g (79.0 mmol) of 2-[(5-nitropyridin-2-yl)amino]ethylamine into 50 mL of tetrahydrofuran, and the mixture was then ice–water cooled. To this cooled mixture was added a solution of 3.80 g (26.0 mmol) of 1-chloroacetylpyrrolidine (**2c**) in 25.0 mL of tetrahydrofuran, via addition funnel, over 40 min. The reaction was then stirred at ice–water temperature for 2 h under a calcium sulfate drying tube and then allowed to stir at room temperature for 18 h. The solvent was then removed in vacuo and the resulting oily paste partitioned between CH₂Cl₂ and water. The aqueous layer was then washed twice with methylene chloride, and the combined organic layers were washed successively with water and brine, dried over sodium sulfate, concentrated, and then purified on silica gel, employing a mixture of 5% methanol in methylene chloride as the eluent to yield the free base as a golden solid. The dihydrochloride salt was obtained following Method A to provide 5.42 g (57% yield) of **8l** a tan solid; mp 220–222 °C; ¹H NMR (D₂O): δ 1.92–2.12 (m, 4H), 3.51 (t, 2H, $J = 5.9$ Hz), 3.58 (t, 4H, $J = 6$ Hz), 4.05 (t, 2H, $J = 6$ Hz), 4.20 (s, 2H), 7.08 (d, 1H, $J = 10$ Hz), 8.48 (d, 1H, $J = 10$ Hz), 9.05 (d, 1H, $J = 1$ Hz); (isobutane/DCI) MH/e 294 (MH⁺) of free base; Anal. (C₁₃H₁₉N₅O₁·2HCl·0.2H₂O·0.2THF) C, H, N.

1-[2-(5-Nitropyridin-2-yl)amino]ethylamino]acetylthiazolidine, Dihydrochloride (8m). A solution of chloroacetyl chloride (2.5 g, 22.0 mmol) in 25 mL of tetrahydrofuran was added dropwise (over 20 min) into an ice–water cold solution containing 2.0 g (22.0 mmol) of thiazolidine (**1d**), 12.4 g (90.0 mmol) of K₂CO₃, and 50 mL of tetrahydrofuran. The reaction was then stirred at ice–water temperature under a calcium

sulfate drying tube for 2 h. The potassium salts were removed via filtration to yield a clear colorless solution of 1-chloroacetylthiazolidine (**2d**) which was immediately taken onto the next step and assumed quantitative (3.7 g). To a 500 mL flask was dissolved 12.1 g (67.0 mmol) of 2-(2-aminoethylamino)-5-nitropyridine into 50 mL of tetrahydrofuran, and the mixture was then cooled in an ice bath. To this cooled mixture was then added a solution of 3.7 g (22.0 mmol) of 1-chloroacetylthiazolidine in the tetrahydrofuran solution (from previous step) dropwise over 30 min. Following the procedure outlined in **8l**, the dihydrochloride salt of **8m** (1.80 g, 25%) was provided as an off-white solid; mp = 203 °C–205 °C; ¹H NMR (D₂O): δ 3.01 (t, 1H, $J = 6.2$ Hz), 3.09 (t, 1H, $J = 6.2$ Hz), 3.37 (t, 2H, $J = 5.2$ Hz), 3.67 (t, 1H, $J = 6.2$ Hz), 3.71 (t, 1H, $J = 6.2$ Hz), 3.79 (t, 2H, $J = 5.9$ Hz), 4.10 (d, 2H, 9.6 Hz), 4.43 (d, 2H, $J = 11.8$ Hz), 6.76 (d, 1H, $J = 9.2$ Hz), 8.30 (dd, 1H, $J = 9.6, 2.6$ Hz), 9.03 (d, 1H, $J = 2.9$ Hz); (ESI-pos) MH/e 312 (MH⁺) of free base; Anal. (C₁₂H₁₇N₅O₃S₁·2HCl) C, H, N.

N-[2-[(5-Cyano-2-pyridinyl)amino]ethyl]glycyl-L-prolinamide (8n). A solution of **2a** (1.00 g, 5.24 mmol) in CH₂Cl₂ (20 mL) was added dropwise over 10 min to an ice–water-cooled mixture of 2-(2-aminoethylamino)-5-cyanopyridine (1.70 g, 10.5 mmol) and K₂CO₃ (2.90 g, 21.0 mmol) in CH₂Cl₂ (40 mL). The reaction was then stirred at ice–water temperature for 2 h and then room temperature for 18 h. The potassium salts were removed via filtration, and the filtrate was concentrated. The residue was chromatographed with 10% CH₃OH in CH₂Cl₂ and then with a 90/10/1 mixture of CH₂Cl₂/CH₃OH/NH₄OH which provided the desired product (558 mg, 34%) as a white solid; mp = 77–80 °C; ¹H NMR (CDCl₃) (2 to 1 ratio of trans/cis amide rotomers): δ 1.86–2.10 (m, 2H), 2.10–2.23 (m, 1H), 2.23–2.32 (m, 1H), 2.82–3.03 (m, 2H), 3.31–3.61 (m, 4H), 3.48 (s, 1.33H, trans conformer), 3.48 (s, 0.66H, cis amide conformer), 3.65–3.57 (m, 1H), 4.47 (dd, 1/3 H, $J = 4.9$ and 2.3 Hz, cis amide conformers), 4.52 (d, t 2/3H, $J = 8.3$ and 2.3 Hz, trans amide conformer), 6.09 (bs, 1/3H, cis amide conformer), 6.34 (bs, 2/3H, trans amide conformer), 6.41–6.52 (m, 1H), 6.45 (d, 2/3H, $J = 9.0$ Hz, trans amide conformer), 6.48 (s, 1/3H, $J = 7.9$ Hz, cis amide conformer), 6.82 (bs, 1/3H, cis amide conformer), 6.93 (bs, 2/3H, trans amide conformer), 6.93 (bs, 2/3H, trans amide conformer), 7.43–7.56 (m, 1H), 8.33 (d, 1H, $J = 2.3$ Hz); (ESI) MH/e 317 (MH⁺) of free base; Anal. (C₁₇H₂₀N₆O₂·0.05H₂O) C, H, N.

1-[3-[[2-[(5-Nitro-2-pyridinyl)amino]ethyl]amino]-1-oxopropyl]-2-cyano-(S)-pyrrolidine, Dihydrochloride (8p). Method A: 2-(2-aminoethylamino)-5-nitropyridine³¹ as amine and **3f** (generated by replacing chloroacetyl chloride with 3-bromopropionyl chloride in the **3a** procedure). Product was a light yellow solid, mp: softens at 80 °C and foams 82–84 °C; ¹H NMR (CD₃OD) (trans and cis amide rotomers in a ratio of 9:1): δ 2.10–2.22 (m, 2H), 2.22–2.32 (m, 2H), 2.90 (t, 2H, $J = 5.6$ Hz), 3.32–3.43 (m, 4H), 3.48–3.60 (m, 1H), 3.65–3.78 (m, 1H), 3.87 (t, 2H, $J = 5.6$ Hz), 4.80 (t, 9/10H, $J = 5.3$ Hz, CHCN), 5.02 (t, 1/10H, $J = 6$ Hz, CHCN), 6.083 (d, 1H, $J = 9.4$ Hz), 8.30 (dd, 1H, $J = 9.4, 2.3$ Hz), 9.04 (dd, 1H, $J = 7.9, 2.6$ Hz); (isobutane/DCI) MH/e 299 (MH⁺) of free base; Anal. (C₁₅H₂₀N₆O₃·2HCl·0.15H₂O·0.35THF) C, H, N.

6-[[2-[(8aS)-hexahydro-1-imino-4-oxopyrrolo[1,2-a]pyrazin-2(1H)-yl]ethyl]amino]-3-pyridinecarbonitrile, Monohydrochloride (8q). A cloudy, white mixture of **8c** as the monohydrochloride³⁰ (0.400 g, 1.20 mmol) and tributylamine (110 mg, 0.60 mmol) in EtOAc (5.00 mL) was heated at reflux for 4 days. The resulting cloudy, white reaction was then filtered from the reaction, washed with EtOAc (10 mL), and dried under reduced pressure to provide a 99/1 mixture of the target product (by HPLC) and starting material, respectively, as a white solid (0.150 g, 45%); mp = 263–265 °C decomp; ¹H NMR (D₂O): δ 1.60–1.76 (m, 1H), 1.82–1.99 (m, 1H), 1.99–2.15 (m, 1H), 2.38–2.50 (m, 1H), 3.12–3.25 (m, 1H), 3.42–3.62 (m, 2H), 3.62–3.90 (m, 3H), 4.05 (d, 1H, $J_{ab} = 16.9$ Hz), 4.37 (d, d 1H, $J_{ab} = 16.9, 2.2$ Hz), 4.97–4.69 (m, 1H), 6.53 (d, 1H, $J = 9.2$ Hz), 7.60 (d, d 1H, $J = 9.2, 1.8$ Hz), 8.21 (d, $J = 1.8$ Hz, 1H); MS *m/z* 299 (MH⁺) of free base; Anal. (C₁₅H₁₈N₆O₁·1.0HCl) C, H, N.

α -(S)-Cyclohexylglycine-2-cyano-(S)-pyrrolidine, Monohydrochloride (9a). This compound was synthesized according to a reported general procedure²⁶ with slight modifications. To a stirring, opaque-white solution of *N*-t-boc-L- α -cyclohexylglycine (2.00 g, 7.77 mmol) and 1-hydroxybenzotriazole hydrate (1.03 g, 7.77 mmol) in CH₂Cl₂ (30 mL) was added *N*-methylmorpholine (2.36 g, 23.3 mmol) and then diisopropylcarbodiimide (2.45 g, 19.4 mmol). After DIC addition, the reaction became clear and then cloudy again after 10 min. At this time, the L-prolinamide (**1a**) (0.890 g, 7.77 mol) was added. The cloudy reaction was then stirred at room temperature for 18 h. The solids were then removed via filtration, and the filtrate was concentrated to provide a golden oil. Purification via chromatography using 3% MeOH/CH₂Cl₂ as eluent provided 1.90 g (69%) of α -(S)-*N*-t-boc-cyclohexylglycine-2-(S)-pyrrolidinecarboxamide. POCl₃ (1.31 mL, 14.0 mmol) was added over 3 min to a CH₃CN/dry ice bath cooled (-35 °C) solution of the above t-boc-protected amide (1.90 g, 5.38 mmol) and imidazole (0.475 g, 7.0 mmol) in dry pyridine (30.0 mL). The reaction was stirred at between -30 °C and -20 °C for 1 h, warmed to room temperature, and then concentrated via rotovap. Purification via chromatography using 3% MeOH in CH₂Cl₂ as eluent provided α -(S)-*N*-t-boc-cyclohexylglycine-2-(S)-pyrrolidinecarbonitrile (0.775 g, 43%) as a white solid; TLC *R*_f: 0.6 (10% MeOH/CH₂Cl₂). A saturated HCl/diethyl ether solution (2.00 mL) was added to a clear, colorless solution of the above t-boc protected nitrile (0.772 g, 2.31 mmol) in diethyl ether (20 mL). The resulting clear, colorless solution was stirred at room temperature for 18 h and then concentrated in vacuo to yield the target compound (0.600 g, 96%) as a white solid: mp = 188–190 °C; ¹H NMR (CD₃OD) (10 to 1 mixture of trans/cis amide rotomers): δ 1.06–1.46 (m, 4H), 1.65–1.99 (m, 7H), 2.04–2.42 (m, 4H), 3.70 (t, 2H, *J* = 6.3 Hz), 4.04 (d, 10/11 H, *J* = 6.3 Hz), 4.26 (d, 1/11H, *J* = 5.1 Hz), 4.84 (dd, 10/11 H, *J* = 7.7 and 5.2 Hz, *CHCN*), 5.06 (dd, 1/11H, *J* = 6.3 and 3.7 Hz, *CHCN*); MS *m/z* 236 (M⁺); Anal. (C₁₃H₂₁N₃O₁·1.0HCl·0.81H₂O·0.09 Et₂O) C, H, N.

1-[(S)-Cyclohexyl(cyclohexylamino)acetyl]-2-cyano-(S)-pyrrolidine (9c). Cyclohexanone (1.60 g, 15.0 mmol) was added to a partially dissolved mixture of **9a** (1.40 g, 5.1 mmol) in 1,2-dichloroethane (56.0 mL). To the ice-water cooled mixture was then added the sodium triacetoxymethylborohydride (2.18 g, 10.0 mmol) in portions over 10 min. The ice-water bath was then removed and the reaction stirred at room temperature for 18 h. The reaction was partitioned between ethyl acetate and water, and the ethyl acetate layer was dried over Na₂SO₄, filtered, and concentrated. Purification via chromatography using 2% CH₃OH in CH₂Cl₂ as eluent provided (0.100 g, 6.3% yield) of the target as a white solid: mp = 78–80 °C; ¹H NMR (CD₃OD) (5 to 1 mixture of trans/cis amide rotomers): δ 1.00–1.35 (m, 10H), 1.55–1.85 (m, 10H), 1.88–1.95 (m, 1H), 2.09–2.22 (m, 2H), 2.22–2.38 (m, 2H), 2.38–2.52 (m, 1H), 3.56–3.67 (m, 2H), 3.69–3.80 (m, 1H), 4.82 (dd, 4/5H, *J* = 8.1 and 4.4 Hz, *CHCN*), 5.17 (dd, 1/5H, *J* = 7.4 and 1.4 Hz, *CHCN*); (ESI) MH/e 318 (MH⁺ of free base); Anal. (C₁₉H₃₁N₃O₁·1.2H₂O·0.2 CH₃OH) C,H; N: calcd, 12.16; found, 11.53.

1-[(2S)-2-Amino-3-methyl-1-oxobutyl]-2-cyano-(S)-pyrrolidine, Monohydrochloride (9d). Same procedure as in **9a** with *N*-t-boc-L-valine as a replacement for *N*-t-boc-L- α -cyclohexylglycine. Product was a white solid; mp 162–164 °C; ¹H NMR (CD₃OD) (trans and cis amide rotomers in a ratio of 9:1) δ 0.98 (d, 1/3H, *J* = 7.0 Hz), 1.08 (d, 3H, *J* = 7.0 Hz), 1.14 (d, 2.67H, *J* = 7.0 Hz), 2.07–2.42 (m, 5H), 3.72 (t, 2H, *J* = 7.0 Hz), 4.10 (d, 1H, *J* = 5.9 Hz), 4.84 (d,d, 9/10 H, *J* = 8.1, 4.8 Hz, *CHCN*), 5.08 (d,d, 1/10H, *J* = 6.2, 3.7 Hz, *CHCN*); (ESI) MH/e 196 (MH⁺ of free base); Anal. (C₁₀H₁₇N₃O₁·1HCl·0.04H₂O·0.14 EtOAc) C, H, N.

1-[(2S)-3-Methyl-2-(methylamino)-1-oxobutyl]-2-cyano-(S)-pyrrolidine, Monohydrochloride (9f). Same procedure as in **9a** with *N*-t-boc-3-methyl-2-methylamino-butyric acid as a replacement for *N*-t-boc-L- α -cyclohexylglycine. Product was a white solid; mp = 223–225 °C; ¹H NMR (CD₃OD) (trans and cis amide rotomers in a ratio of 9:1) δ 1.10 (d, 3H, *J* = 7.0 Hz),

1.16 (d, 3H, *J* = 7.0 Hz), 2.10 (m, 5H), 2.69(s, 2.7 H), 2.71 (s, 0.3H), 3.65–3.82 (m, 2H), 4.18 (d, 1H, *J* = 5.15 Hz), 4.89 (d,d, 0.9H, *J* = 8.1, 4.4 Hz, *CHCN*), 5.08(d,d, 0.1H, *J* = 7.0, 2.6 Hz, *CHCN*). ¹³CNMR (CD₃OD): δ 17.73, 18.59, 26.22, 30.73, 31.26, 33.29, 66.08, 119.14, 119.70, 167.53. (ESI) MH/e 210 (MH⁺ of free base). Anal.(C₁₁H₁₉N₃O₁·1HCl), C, H, N.

1-(3-Cyclohexyl-1-oxopropyl)-2-cyano-(S)-pyrrolidine (9g). To a cloudy solution of 3-cyclohexanepropionic acid (1.0 g, 6.40 mmol) and L-prolinamide (**1a**) (730 mg, 6.40 mmol) in CH₂Cl₂ (25 mL) were added DMAP (20 mg) and DIC (890 mg, 7.04 mmol). The initially clear reaction was stirred for a total of 6 h to provide a cloudy white mixture. The solids were removed via filtration, and the filtrate was concentrated to provide a white solid. Purification via chromatography using 3% CH₃OH in CH₂Cl₂ as eluent provided 1-(3-cyclohexyl-1-oxopropyl)-(S)-prolinamide (1.37 g, 5.44 mmol) as a white solid. To an ice-water cooled solution of this amide (1.37 g, 5.44 mmol) in CH₂Cl₂ (25 mL) was slowly added TFAA (1.54 mL, 10.9 mmol) over 10 min and then stirred at ice-water temperature for 2 h. The reaction was then partitioned between methylene chloride and saturated aqueous sodium bicarbonate, and the aqueous layer was washed twice with methylene chloride. The combined organic layers were then washed successively with water and brine and then dried over sodium sulfate. Purification via chromatography using 40% EtOAc in hexane as eluent provided the desired product (871 mg, 69%) as a white solid; mp = 40–42 °C; ¹H NMR (CDCl₃) (7 to 1 mixture of trans/cis amide rotomers): δ 0.82–1.02 (m, 2H), 1.11–1.33 (m, 4H), 1.51–1.63 (m, 2H), 1.63–1.77 (m, 5H), 2.07–2.25 (m, 2H), 2.25–2.40 (m, 4H), 3.41–3.52 (m, 1H), 3.57–3.70 (m, 1H), 4.59 (dd, 1/8 H, *J* = 8.1 and 1.8 Hz, *CHCN*), 4.75 (d, 7/8H, *J* = 7.7, 2.2 Hz, *CHCN*); (ESI) MH/e 235 (MH⁺ of free base). Anal. (C₁₄H₂₂N₂O₁) C, H, N.

1-[(1-Adamantyl)amino]acetylpyrrolidine, Monohydrochloride (12c). To an ice-water cooled mixture of 1-aminoadamantane (15.9 g, 105.0 mmol), K₂CO₃ (19.4 g, 140 mmol) and CH₂Cl₂ (168 mL) was added a solution of ethyl bromoacetate (5.17 mL, 140 mmol) and CH₂Cl₂ (50 mL) dropwise over 20 min. The resulting cloudy, yellow-white mixture was then stirred at ice-water temperature for 1.5 h, then at RT for 18 h and then filtered through a plug of Celite (50 g). The solids and Celite plug were then washed with 100 mL of CH₂Cl₂, and the combined organic fractions were concentrated in vacuo to provide a cloudy, yellow-white oil. Purification via chromatography (4/1 mixture of hexane/ethyl acetate as eluent) followed by concentration in vacuo provided 6.9 g (83% yield) of ester **4** as a white solid. To an ice-water cooled mixture of ester **4** (6.87 g, 28.9 mmol), K₂CO₃ (15.9 g, 115 mmol), and CH₂Cl₂ (80 mL) was added a solution of benzyl chloroformate (4.34 mL, 30.4 mmol) in CH₂Cl₂ (26 mL) over 15 min. The resulting cloudy, white mixture was then stirred at ice-water temperature for 1.5 h, then at RT for 18 h, filtered, and concentrated in vacuo to provide a white crunchy solid. Purification via chromatography (9/1 mixture of hexane/ethyl acetate as eluent) followed by concentration in vacuo provided 7.89 g (73.6% yield) of CBZ-protected **4** as a white solid. A solution of this CBZ-protected **4** (7.89 g, 21.3 mmol), THF/H₂O: 1/1 (85 mL), and LiOH·H₂O (7.14 g, 170 mmol) was stirred at 50 °C for 22h, cooled to RT, and poured into a 303 mL mixture of EtOAc/H₂O/AcOH (200/100/3 ratio). The organic layer is then isolated, washed with 2 × 50 mL of H₂O, dried over MgSO₄, filtered, and concentrated in vacuo to provide (6.7 g, 92%) of acid **5** as an off-white solid. To a solution of acid **5** (0.500 g, 1.46 mmol) in CH₂Cl₂ (20 mL) were added HOBT (0.195 g, 1.46 mmol), NMM (0.440 g, 4.37 mmol), and finally DIC (0.460 g, 3.64 mmol). After stirring at room temperature for 10 min, pyrrolidine (0.195 g, 1.46 mmol) was added to the cloudy-white solution via syringe, and the reaction was stirred at RT for 18 h. A CH₂Cl₂/NaHCO₃(aq) workup and purification via chromatography (40% EtOAc in hexane as eluent) provided 0.428 g (74% yield) of the CBZ-protected **12c** as a white solid. Deprotection of this intermediate was accomplished by shaking 0.428 g (1.08 mmol) of the CBZ-protected **12c** in a solution of EtOAc (50 mL), 10% Pd/C (0.100 g) and H₂ (1atm) at RT for

18 h. The solution was filtered through Celite and concentrated in vacuo to yield the free base of **12c** as a clear oil. HCl gas was gently bubbled into a solution of this free base in THF (25 mL) for ~20 s stirred at RT for 15 min and then concentrated in vacuo to provide the monohydrochloride salt of **12c** as a white solid (63% yield from **5**); mp 242 °C, sublimes; ¹H NMR (D₂O) δ 1.67 (bq, 6H, *J*_{ab} = 16.5 Hz), 1.89 (s, 6H), 1.80–2.00 (m, 4H), 2.16 (bs, 3H), 3.40 (q, 4H, *J* = 6.3 Hz), 3.87 (s, 2H); (ESI) MH/e 263 (MH⁺ of free base); Anal. (C₁₆H₂₆N₂O₁·1HCl·0.5H₂O·0.1THF) C, H, N.

1-[[1-(1-Adamantyl)amino]acetyl]azetidide (12d). Following procedure for **12c** but replacing pyrrolidine with azetidide as the amine. Product was a white solid (67% yield from **5**); mp 65–67 °C; ¹H NMR (CDCl₃): δ 1.52–1.72 (m, 10H), 1.85 (bs, 2H), 2.05 (bs, 3H), 2.22–2.35 (m, 2H), 3.18 (s, 2H), 4.06 (t, 2H, *J* = 7.7 Hz), 4.12 (t, 2H, *J* = 7.7 Hz); (ESI) MH/e 249 (MH⁺ of free base); Anal. free base (C₁₅H₂₄N₂O₁·0.06H₂O) C, H, N.

1-[[1-(1-Adamantyl)amino]acetyl]piperidine (12e). Following procedure for **12c** but replacing pyrrolidine with piperidine as amine. Product was a white solid (68% yield from **5**); mp 80–82 °C; ¹H NMR (CDCl₃): δ 1.48–1.70 (m, 18H), 2.03 (bs, 3H), 3.10 (t, 2H, *J* = 5.1 Hz), 3.40 (s, 2H), 3.52 (t, 2H, *J* = 5.1 Hz); (ESI) MH/e 277 (MH⁺ of free base); Anal. (C₁₇H₂₈N₂·O₁·0.1EtOAc) C, H, N.

1-[[1-(1-Adamantyl)amino]acetyl]-3-pyrrolidinol, Monohydrochloride (12f). Following procedure for **12c** but replacing pyrrolidine with 3-pyrrolidinol as amine. Product was a white solid (51% yield from **5**); mp 230–232 °C; ¹H NMR (D₂O): (3 to 2 ratio of amide rotomers: δ 1.65 (q, 6H, *J* = 16.5 Hz), 1.87 (s, 6H), 1.91–2.10 (m, 2H), 2.15 (s, 3H), 3.37–3.63 (m, 3H), 3.83–3.97 (m, 2H), 4.47 (bs, 0.6H, OH of one amide rotomer), 4.54 (bs, 0.4H, OH of other amide rotomer); (ESI) MH/e 279 (MH⁺ of free base); Anal. (C₁₆H₂₆N₂O₂·1.0HCl·0.95H₂O·0.35THF) C, H, N.

1,2,3,4-Tetrahydro-2-[[1-(1-Adamantyl)amino]acetyl]-isoquinoline, monohydrochloride (12g). Following procedure for **12c** but replacing pyrrolidine with 1,2,3,4-tetrahydroisoquinoline as amine. Product was a white solid (53% yield from **5**); mp = 260–262 °C; ¹H NMR (D₂O) (1 to 1 trans to cis amide rotomers) δ 1.65 (bq, 6H, *J* = 15.3 Hz), 1.86 (s, 6H), 2.13 (bs, 3H), 2.84 (t, 1H, *J* = 6 Hz), 2.91 (t, 1H, *J* = 6 Hz), 3.62–3.75 (m, 2H), 4.05 (s, 2H, one rotomer), 4.06 (s, 2H, other rotomer), 4.59 (s, 1H, one amide rotomer), 4.63 (s, 1H, other amide rotomer), 7.15–7.25 (m, 4H); (ESI) MH/e 325 (MH⁺ of free base); Anal. (C₂₁H₂₈N₂O₁·1HCl·0.896H₂O·0.14THF) C, H, N.

1-[[3-(3-Hydroxy-1-Adamantyl)amino]acetyl]-2-cyano-(S)-pyrrolidine (12j). Method A: 3-hydroxy-1-aminoadamantane³² as amine and use of **3a**. Product was a white solid; mp: 138–140 °C (when recrystallized from EtOAc and 2-propanol: mp: 148–150 °C); OR: [d] = –78.3° (*c* = 9.73, MeOH); ¹H NMR (CDCl₃) (5 to 1 mixture of trans to cis amide rotomers): δ 1.47–1.79 (m, 12H), 1.67 (s, 3H), 2.05–2.25 (m, 2H), 2.25–2.38 (m, 4H), 3.40–3.54 (m, 1H), 3.45 (d, 2H, *J* = 1.9 Hz), 3.57–3.67 (m, 1H), 4.77 (dd, 5/6H, *J* = 7.5, 2.3 Hz, *CHCN*), 4.86 (dd, 1/6H, *J* = 7.9, 1.9 Hz, *CHCN*); (ESI) MH/e 304 (MH⁺ of free base); Anal. (C₁₇H₂₅N₃O₂) C, H, N.

N-(3-Hydroxy-1-Adamantyl)glycyl-L-prolinamide (12k). Following procedure for **8n** and using 3-hydroxy-1-aminoadamantane³² as amine. Product was a white, hygroscopic solid; mp = 94–96 °C; ¹H NMR (DMSO): (trans and cis amide rotomers in a ratio of 2:1) δ 1.24–1.54 (m, 10H), 1.54–1.63 (m, 3H), 1.70–2.01 (m, 4H), 2.11 (bs, 2H), 2.17 (bs, 1H), 3.17 (s, 4/3H), 3.32 (s, 2/3H), 3.36–3.47 (m, 1H), 3.47–3.59 (m, 1H), 4.18 (dd, 2/3H, *J* = 9.2 and 2.9 Hz), 4.30 (dd, 1/3H, *J* = 8.4 and 2.9), 6.92 (bs, 2/3H, amide), 7.18 (bs, 1/3H, amide), 7.28 (bs, 2/3H, amide), 7.57 (bs, 1/3H, amide); IR (KBr): 1640.4, 1677.3 (cm⁻¹); (ESI) MH/e 322 (MH⁺ of free base); Anal. (C₁₇H₂₇N₃O₃·1.5H₂O·0.22 CH₃OH) C, H, N.

N-(3-Hydroxy-1-Adamantyl)glycyl-L-proline, Monotri-fluoroacetic Acid (12l). Following the procedure for **2a**, L-proline-*tert*-butyl ester (**1e**) was coupled with chloroacetyl chloride to provide **2e** (golden oil) which was then coupled with 3 equiv of 3-hydroxy-1-aminoadamantane³² following the

procedure for **8n**. Purification with chromatography (4% MeOH in CH₂Cl₂ as eluent) provided a 42% yield over two steps of the *t*-boc ester of **12l** as a light yellow solid. Cleavage of the *t*-boc ester was obtained by stirring at room temperature with 2 equiv of TFA in 0.5 M solution of CH₂Cl₂ overnight. The resulting TFA salt of **12l** was obtained as a white, hygroscopic solid in a 92% yield upon concentration in vacuo; mp = 80–82 °C; ¹H NMR (CD₃OD) (4 to 1 mixture of trans to cis amide rotomers): δ 1.62 (s, 2H), 1.73 (s, 4H), 1.81–1.91 (m, 2H), 1.89 (s, 4H), 2.01–2.14 (m, 2H), 2.24–2.40 (m, 2H), 2.40 (s, 2H), 3.54–3.73 (m, 2H), 4.01 (s, 2H), 4.49 (d, d, 4/5H, *J* = 8.8, 3.3 Hz, *CHCN*), 4.69 (d, d, 1/5H, *J* = 8.5, 2.6 Hz, *CHCN*); (ESI) MH/e 435 (MH⁺ of free base); Anal. (C₁₇H₂₆N₂O₃·1.3TFA·0.28H₂O) C, H, N. **Note:** An excess 0.3 equiv of TFA could not be removed even with several toluene chases, triturations with Et₂O, and high vacuum (~1 mm) over several days.

1-[[[3-[[*tert*-Butylamino]carbonyloxy]-1-Adamantyl]amino]acetyl]-2-cyano-(S)-pyrrolidine; Monohydrochloride (12m). To a mixture of 1-aminoadamantane-3-ol³² (5.00 g, 30 mmol) and potassium carbonate (6.20 g; 45 mmol) in 150 mL of THF was added benzyl chloroformate (4.70 g, 33.0 mmol) in dropwise fashion over a 10 min period. The mixture was then stirred at RT for 2 h and then partitioned between ethyl acetate and water. The aqueous layer was washed twice with ethyl acetate (100 mL), and the combined organic layers were then washed successively with 100 mL of aqueous 2 N sodium hydroxide, water, and brine, dried over sodium sulfate, filtered, and concentrated in vacuo to provide (8.03 g, 85% yield) of 1-benzylcarbamoyladamantane-3-ol (**6**) as a white solid. To a clear solution of 1-benzylcarbamoyladamantane-3-ol (**6**) (1.00 g, 3.32 mmol) and *tert*-butyl isocyanate (380 μL, 3.32 mmol) in 30 mL of CH₂Cl₂ was then syringe-added TMSCl (20.0 μL, 0.17 mmol). This reaction was then stirred at RT for 18 h, concentrated in vacuo, and purified on silica gel with 20% ethyl acetate in hexane as eluent to yield 3-[[*tert*-butylamino]carbonyloxy]-1-benzylcarbamoyladamantane (**7a**) as a white solid in quantitative yield. A mixture of 3-[[*tert*-butylamino]carbonyloxy]-1-benzylcarbamoyladamantane (1.50 g, 3.75 mmol) and 10% palladium on carbon (400 mg) in ethanol (150 mL) was then shaken under hydrogen (50 psi) for 24 h, filtered through Celite, and concentrated in vacuo to provide 3-[[*tert*-butylamino]carbonyloxy]-1-aminoadamantane as a clear oil in 99% yield. Method A was then followed using 3-[[*tert*-butylamino]carbonyloxy]-1-aminoadamantane as the amine to provide **12m** as a yellow solid; mp: 210–212 °C; ¹H NMR (CD₃OD) (9 to 1 mixture of trans to cis amide rotomers): δ 1.26 (s, 9H), 1.62–1.71 (m, 2H), 1.92 (s, 4H), 1.98–2.44 (m, 12H), 3.51–3.62 (m, 1H), 3.70–3.78 (m, 1H), 4.04 (d, 2H, *J* = 6.6 Hz), 4.82 (t, 9/10H, *J* = 5.5 Hz, *CHCN*), 5.07 (d, d, 1/10H, *J* = 6.6, 2.9, *CHCN*); (ESI) MH/e 403 (MH⁺ of free base); Anal. (C₂₂H₃₄N₄O₃·1.0HCl·0.67H₂O·0.40THF) C, H, N, Cl.

1-[[[3-[[4-Methoxyphenyl]amino]carbonyloxy]-1-Adamantyl]amino]acetyl]-2-cyano-(S)-pyrrolidine; Monohydrochloride (12n). The procedure for **12m** was followed except in the second step to form **7b** where an equivalent of 4-methoxyphenyl isocyanate replaces *tert*-butyl isocyanate, 1,2-dichloroethane was used as solvent instead of methylene chloride, and the reaction is stirred at 50 °C for 18 h. Product was provided as a yellow solid (55% yield from **7b**); mp: 212–214 °C; ¹H NMR (CD₃OD) (9 to 1 mixture of trans to cis amide rotomers): δ 1.63–1.79 (m, 2H), 1.94 (s, 4H), 2.08–2.34 (m, 8H), 2.46 (s, 4H), 3.51–3.62 (m, 2H), 3.75 (s, 3H), 4.07 (d, 2H, *J* = 7.0 Hz), 4.82 (t, 9/10H, *J* = 5.8 Hz, *CHCN*), 5.09 (d, d, 1/10H, *J* = 7.0, 2.2, *CHCN*), 6.83 (d, d, 2H, *J* = 8.8, 1.1 Hz), 7.27 (d, 2H, *J* = 8.4 Hz); (ESI) MH/e 453 (MH⁺ of free base); Anal. (C₂₅H₃₂N₄O₄·1.0HCl·1.15H₂O·0.55THF) C, H, N, Cl.

1-[[[3-[[Phenylamino]carbonyloxy]-1-Adamantyl]amino]acetyl]-2-cyano-(S)-pyrrolidine; Monohydrochloride (12o). The procedure for **12m** was followed except in the second step to form **7c** where an equivalent of phenyl isocyanate replaces *tert*-butyl isocyanate, 1,2-dichloroethane was used as solvent instead of methylene chloride, and the reaction was stirred at 50 °C for 18 h. Product was a light yellow solid (48% yield from **7c**); mp = 205–207 °C; ¹H NMR (CD₃OD) (9

to 1 mixture of trans to cis amide rotomers): δ 1.62–1.81 (m, 2H), 1.97 (s, 4H), 2.10–2.32 (m, 8H), 2.47 (s, 4H), 3.51–3.62 (m, 2H), 4.06 (d, 2H, $J = 7.0$ Hz), 4.82 (t, 9/10H, $J = 5.9$ Hz, *CHCN*), 5.08 (d,d, 1/10H, $J = 7.0$ and 2.2 Hz, *CHCN*), 6.99 (d,d,d, 1H, $J = 7.0, 7.0, 1.1$ Hz), 7.24 (d,d,d, 2H, $J = 7.4, 7.4, 2.2$ Hz), 7.37 (d, 2H, $J = 8.8$ Hz); (ESI) MH/e 423 (MH⁺ of free base); Anal. (C₂₄H₃₀N₄O₃·1.0HCl·1.06H₂O·0.64THF) C, H, N.

1-[[[3-[[[(Diisopropyl)amino]carbonyl]-oxy]-1-adamantyl]amino]acetyl]-2-cyano-(S)-pyrrolidine; Monohydrochloride (12p). The procedure for **12m** was followed except in the second step to form **7d** where an equivalent of diisopropylcarbonyl chloride replaces *tert*-butyl isocyanate, 1,2-dichloroethane was used as solvent instead of methylene chloride, and the reaction was stirred at 50 °C for 18 h. Product was a white solid (63% yield from **7d**); mp: 148–150 °C; ¹H NMR (CD₃OD) (8 to 1 mixture of trans to cis amide rotomers): δ 1.21 (bs, 12H), 1.61–1.78 (m, 2H), 1.95 (s, 4H), 2.04–2.36 (11H, m), 2.36–2.48 (m, 4H), 3.50–3.61 (m, 1H), 4.06 (d, 2H, $J = 7.4$ Hz), 4.82 (t, 8/9H, $J = 5.9$ Hz, *CHCN*), 5.09 (d,d, 1/9H, $J = 7.0, 2.6$ Hz, *CHCN*); (ESI) MH/e 431 (MH⁺ of free base); Anal. (C₂₄H₃₆N₄O₃·1.0HCl·1.2H₂O·0.40THF) C, H, N.

1-[[[3-[[[(Cyclohexyl)amino]carbonyl]-oxy]-1-adamantyl]amino]acetyl]-2-cyano-(S)-pyrrolidine; Monohydrochloride (12q). The procedure for **12m** was followed except in the second step to form **7e** where an equivalent of cyclohexyl isocyanate replaces *tert*-butyl isocyanate, 1,2-dichloroethane was used as solvent instead of methylene chloride, and the reaction was stirred at 50 °C for 18 h. Product was provided as a light brown solid (41% yield from **7e**); mp: 155–157 °C; ¹H NMR (CD₃OD) (9 to 1 mixture of trans to cis amide rotomers): δ 1.08–1.40 (m, 6H), 1.56–1.78 (m, 5H), 1.78–1.98 (m, 6H), 1.98–2.47 (m, 12H), 3.43–3.61 (m, 2H), 4.04 (d, 2H, $J = 7.0$ Hz), 4.83 (t, 9/10 H, $J = 5.9$ Hz, *CHCN*), 5.09 (dd, 1/10H, $J = 7.5, 1.8$, *CHCN*); (ESI) MH/e 429 (MH⁺ of free base); Anal. (C₂₄H₃₆N₄O₃·1.0HCl·0.77H₂O·0.32THF) C, H, N.

1-[[[3-Acetyloxy-1-adamantyl]amino]-acetyl]-2-cyano-(S)-pyrrolidine; Monohydrochloride (12r). The procedure for **12m** was followed except in the second step where a standard acylation of **6** is performed using 1.2 equiv of acetyl chloride, 3.0 equiv of pyridine, 0.1 equiv of DMAP, and 1,2-dichloroethane which are all stirred at room temperature for 24 h. Product obtained was a light yellow taffy (45% yield from **7f**); ¹H NMR (CD₃OD) (6 to 1 mixture of trans to cis amide rotomers): δ 1.55–1.72 (6H, m), 1.94 (s, 3H), 1.98–2.34 (m, 13H), 3.42–3.58 (m, 1H), 3.44 (d, 1H, $J = 6.6$ Hz), 3.62–3.75 (m, 1H), 4.77 (t, 6/7H, $J = 5.5$ Hz, *CHCN*), 5.09 (d,d, 1/7H, $J = 6.6$ and 3.3 Hz, *CHCN*); (ESI) MH/e 346 (MH⁺ of free base); Anal. (C₁₉H₂₇N₃O₃·0.38H₂O) C, H, N.

In Vitro Studies. DPP-IV Inhibition Measurement in Vitro: Caco-2 Assay. An extract from human colonic carcinoma cells (Caco-2; American Type Culture Collection; ATCC HTB 37) was used as the source of DPP-IV in the assay. The cells were differentiated to induce DPP-IV expression as described by previously.⁴² Cell extract was prepared from cells solubilized in lysis buffer (10 mM Tris-HCl, 0.15 M NaCl, 0.04 T.I.U. (trypsin inhibitor unit) aprotinin, 0.5% nonidet-P40, pH 8.0) then centrifuged at 35 000g for 30 min at 4 °C to remove cell debris. The assay was conducted by adding 20 μ g of solubilized Caco-2 protein, diluted to a final volume of 125 μ L in assay buffer (25 mM Tris-HCl pH 7.4, 140 mM NaCl, 10 mM KC1, 1% bovine serum albumin) to 96-well flat-bottom microtiter plates. The reaction was initiated by adding 25 μ L of 1 mM substrate (H-Ala-Pro-pNA; pNA is *p*-nitroaniline). The reaction was run at room temperature for 10 min, and then 19 μ L of 25% glacial acetic acid was added to stop the reaction. Fluorescence was measured using a CytoFluor II fluorometer (excitation 380 nm/ emission 460 nm). Test compounds and solvent controls were added as 30 μ L additions, and the assay buffer volume was reduced to 95 μ L. A standard curve of free *p*-nitroaniline was generated using 0–100 μ M pNA in assay buffer. The curve generated, which was linear, was used for interpolation of substrate consumption (catalytic activity in nmoles substrate cleaved /min).

DPP-IV Inhibition Measurement ex Vivo. Rat, Human, Monkey Plasma Assays. Human, rat, or monkey plasma was used as the source of DPP-IV in the assay. The standard assay was modified from a previously published method.⁴³ Five μ L of plasma was added to 96-well flat-bottom microtiter plates, followed by the addition of 5 μ L of 80 mM MgCl₂ in assay buffer (25 mM HEPES, 140 mM NaCl, 1% RIA-grade BSA, pH 7.8). After a 5-min preincubation at room temperature, the reaction was initiated by the addition of 10 μ L of assay buffer containing 0.1 mM substrate (H-Gly-Pro-AMC; AMC is 7-amino-4-methylcoumarin). The plates were covered with aluminum foil (or kept in the dark) and incubated at room temperature for 20 min. After incubation, fluorescence was measured using a CytoFluor II fluorometer (excitation 380 nm/ emission 460 nm). Test compounds and solvent controls were added as 2 μ L additions, and the assay buffer volume was reduced to 13 μ L. A standard curve of free AMC was generated using 0–50 μ M solutions of AMC. The curve generated, which was linear, was used for interpolation of substrate consumption (catalytic activity in nmoles substrate cleaved /min).

DPP-II Inhibition Measurement in Vitro. An extract of bovine kidney homogenate, partially purified by ion-exchange and adenosine deaminase chromatography, was used as the source of DPP-II in the assay.^{44–46} The standard assay was modified from a previously published method.⁴⁷ Twenty micrograms of DPP-II-containing fraction diluted to a final volume of 60 μ L in assay buffer (0.2 M Borate, 0.05 M Citrate, pH 5.3) was added to 96-well flat-bottom microtiter plates, followed by the addition of 10 μ L of 10 mM *o*-phenanthroline (to inhibit aminopeptidase activity) and 20 μ L of 5 mM substrate (H-Lys-Ala-AMC; AMC is 7-amino-4-methylcoumarin). The plates were incubated at 37 °C for 30 min. After incubation, fluorescence was measured using a CytoFluor II fluorometer (excitation 380 nm/ emission 460 nm). Test compounds and solvent controls were added as 20 μ L additions, and assay buffer volume is reduced to 50 μ L. A standard curve of AMC was generated using 0 to 100 μ M of AMC. The curve generated, which was linear, was used for interpolation of catalytic activity (in nmoles substrate cleaved/min).

Post-Proline Cleaving Enzyme (PPCE) Inhibition Measurement in Vitro. A cytosolic extract of human erythrocytes, partially purified by ion-exchange chromatography, was used as the source of PPCE in the assay. The standard assay is modified from a previously published method.⁴⁸ PPCE-containing fraction (350 ng protein) diluted to a final volume of 90 μ L in assay buffer (20 mM NaPO₄, 0.5 mM EDTA, 0.5 mM DTT, 1% BSA, pH 7.4) was added to 96-well flat-bottom microtiter plates, followed by the addition of 10 μ L of 0.5 mM substrate (Z-Gly-Pro-AMC; AMC is 7-amino-4-methylcoumarin). The plates were incubated at room temperature for 30 min. After incubation, fluorescence was measured using a CytoFluor II fluorometer (excitation 380 nm/ emission 460 nm). Test compounds and solvent controls were added as 20 μ L additions, and the assay buffer volume was reduced to 70 μ L. A standard curve of free AMC was generated using 0 to 5 μ M solutions of AMC. The curve generated, which was linear, was used for interpolation of catalytic activity (in nmoles substrate cleaved/min).

In Vivo Obese Male (fa/fa) Zucker Rat Studies. Effect of 12j on DPP-IV Activity, Active GLP-1 Levels, and Glucose and Insulin Excursions. Studies were performed on obese male Zucker (fa/fa) rats (Charles River Labs, Cambridge, MA); controls ($n = 9$) and **12j**-treated ($n = 9$). These rats were purchased at 7 weeks of age, cannulated at 7.5 weeks, and studied beginning at around 11 weeks of age. In the morning of the oral glucose tolerance test (OGTT), the rats were “fasted” by removing food before the lights were turned on, after which they were transferred to the experiment room at 8:00 a.m.. **12j** was dissolved in vehicle solution (0.5% carboxymethylcellulose (CMC) and 0.2% Tween 80). The cannulas were connected to sampling tubing (PE-100, 0.034 in. i.d. \times 0.06 in. o.d.), which were filled with saline. After 30–40 min cage acclimation, a 0.5 mL baseline blood sample was taken at $t = -15$ min, and the rats were then orally dosed

with CMC or **12j** (10 $\mu\text{mol/kg}$), after which additional baseline blood samples were taken at $t = -5, -2.5,$ and 0 min. The animals were then administered an oral glucose solution (10% glucose, 1 g/kg) immediately after $t = 0'$. The rest of the samples were taken at 1, 3, 5, 10, 15, 20, 30, 45, 60, 75, and 90 min. Throughout the OGTT, an equal volume of donor blood was used to replace the blood withdrawn during sampling. Donor blood was obtained from donor rats through cardiac puncture. The collected blood samples (0.5 mL) were immediately transferred into chilled Eppendorf tubes containing 50 μL of EDTA: trasyolol (25 mg/mL of 10 000 trasyolol (FBA Pharmaceuticals)) and used for the measurement of glucose and insulin levels and DPP-IV activity. Larger blood samples (0.75 mL) were collected at $t = -15, 0, 5, 10, 15,$ and 30 min for GLP-1 (7–36 amide) measurements. To these tubes, the DPP-IV inhibitor valine pyrrolidide⁴⁹ was added to yield a final concentration in the blood of 1 μM . Technical difficulties with obtaining blood samples after minute 20 for one rat in both the CMC and **12j** groups resulted in the inability to calculate glucose and insulin AUC data for those rats, leading to AUC data with an $n = 8/\text{group}$. Measurement of plasma glucose was made using a modification of a Sigma Diagnostics glucose oxidase kit. DPP-IV activity was measured in plasma samples obtained at $-5, 0, 20, 45,$ and 90 min DPP-IV activity as previously described in the above ex vivo rat plasma experimental. Plasma levels of GLP-1 (7–36 amide) were measured using the GLP-1 (active) Elisa Kit (Linco Research Cat# EGLP-35K, St. Charles, MO). A double antibody RIA method using a rat-specific antiinsulin antibody from Linco Research (#1013, lot # ARI-02 (16T), St. Charles, MO) was used to measure plasma insulin. All data were expressed as the mean \pm SEM for each experimental group of rats. Statistical analysis of data was performed using a two-tailed unpaired Student's t -test (Microsoft Excel 5.0), or a two-way repeated measures ANOVA with a Tukey post-ANOVA test (SPSS Inc. SigmaStat for windows, version 2.03).

In Vivo Cynomolgus Monkey PK/PD Studies Using **8c and **12j**.** Ketamine-anesthetized male healthy cynomolgus monkeys received either **8c** ($n = 2$) or **12j** ($n = 3$) (dissolved in CMC/Tween-80) by oral gavage (1.007 $\mu\text{mol/kg}$), and by intravenous administration (0.399 $\mu\text{mol/kg}$) (dissolved in saline). For iv study, compound was administered (0.4 mL/kg over 1 min) in 0.9% saline as vehicle. Different monkeys were used for each dosage regimen. Basal blood samples were collected at -10 min and immediately prior to administration of compound. Blood samples were collected at 0.03, 0.08, 0.17, 0.25, 0.33, 0.42, 0.5, 0.75, 1, 1.25, 1.5, 2, 2.5, 3, 3.5, 4, 7, 12, and 25 h postdose for both routes of administration. Blood was obtained into heparin-coated syringes, transferred to microcentrifuge tubes, and centrifuged to separate the plasma. The plasma was stored at -80 $^{\circ}\text{C}$ in fresh microcentrifuge tubes until assay. DPP-IV activity was measured in a similar manner as previously described in the above ex vivo rat and human plasma experimentals. Plasma DPP-IV activities were calculated and expressed as 'percent of baseline' to reduce variability due to individual differences in plasma enzyme activity. Area-under-curve (AUC) values for DPP-IV activity were calculated from time (hours after dose) vs effect (percent inhibition) curves from individual animals using the trapezoidal method. The ratio of dose-normalized effect AUC for oral/intravenous administration routes was taken as an estimate of effect bioavailability. Parent drug concentrations were determined using an HPLC/MS/MS method with a limit of quantification of 1 ng/mL. Pharmacokinetic parameters were calculated using noncompartment modeling, and the AUC was calculated using the linear trapezoidal method. Absolute oral bioavailability was calculated by $(\text{AUC}_{0-\infty\text{po}} \times 399)/(\text{AUC}_{0-\infty\text{iv}} \times 1007)$.

Acknowledgment. The authors thank Dr. Phillip E. Fanwick from Purdue University for conducting the X-ray crystallographic analysis of **12j**. The authors thank Eric M. Loeser for monohydrochloride of **8q**, George T. Lee for a generous quantity of a key inter-

mediate, Elina Dunn, Huiping H. Gu, Lori A. Bolognese, Xue Li, Wieslawa M. Maniara, Michele Valentin, and Stephen C. Weldon for their assistance in the in vivo analysis of **12j**, and Robert C. Anderson and Philip A. Bell for helpful discussions. We also thank Dr. Gregory Bebernitz for helpful comments while reviewing this manuscript.

Supporting Information Available: ORTEP drawing and atomic coordinate information for **12j** and experimental details for **8b, 8d–j, 8o, 9b, 9e, 9h, 10a–h, 11a–ak, 12a,b,** and **12h–i**. This material is available free of charge via the Internet at <http://pubs.acs.org>.

References

- (1) (a) Yaron, A.; Nadier, F. Proline-Dependent Structural and Biological Properties of Peptides and Proteins. *Crit. Rev. Biochem. Mol. Biol.* **1993**, *28*, 31–81. (b) Demuth, H.; Heins J. Catalytic mechanism of Dipeptidyl Peptidase-IV. In *Dipeptidyl Peptidase-IV (CD26) in Metabolism and the Immune Response*; Fleischer, B., Ed.; Landes, R. G.: Austin, TX, 1995; Vol. 3, pp 1–35.
- (2) Mentlein, R. Dipeptidyl-peptidase IV (CD26)-role in the inactivation of regulatory peptides. *Regul. Pept.* **1999**, *85*, 9–24.
- (3) (a) Jacotot, E.; Callebaut, C.; Blanco, J.; Krust, B.; Neubert, K.; Barth, A.; Hovanessian, A. G. Dipeptidyl-peptidase IV-B, a novel form of cell-surface-expressed protein with dipeptidyl-peptidase IV activity. *Eur. J. Biochem.* **1996**, *239*, 248–258. (b) Schneider, B. L.; Thevananthar, S.; Moyer, M. S.; Walters, H. C.; Rinaldo, P.; Devarajan, P.; Sun, A. Q.; Dawson, P. A.; Ananthanarayanan, M. Cloning and Characterization of a Novel Peptidase from Rat and Human Ileum. *J. Biol. Chem.* **1997**, *272*, 31006–31015. (c) Duke-Cohan, J. S.; Gu, J.; McLaughlin, D. F.; Xu, Y.; Freeman, G. J.; Schlossman, S. F. Attractin (DPPT-L), a member of the CUB family of cell adhesion and guidance proteins, is secreted by activate human T lymphocytes and modulate immune cell interactions. *Proc. Natl. Acad. Sci. U.S.A.* **1998**, *95*, 11336–11341. (d) Niedermeyer, J.; Enenkel, B.; Park, J. E.; Lenter, M.; Rettig, W. J.; Damm, K.; Schnapp, A. Mouse fibroblast-activation protein-conserved *Fap* gene organization and biochemical function as a serine protease. *Eur. J. Biochem.* **1998**, *254*, 650–654. (e) Chiravuri, M.; Schmitz, T.; Yardley, K.; Underwood, R.; Dayal, Y.; Huber, B. T. A Novel Apoptotic Pathway in Quiescent Lymphocytes Identified by Inhibition of a Post-Proline Cleaving Aminodipeptidase: A Candidate Target Protease, Quiescent Cell Proline Dipeptidase. *J. Immunol.* **1999**, *163*, 3092–3099.
- (4) (a) Holst, J. J. Glucagon-like peptide-1 (GLP-1) a newly discovered GI hormone. *Gastroenterology* **1994**, *107*, 1048–1055. (b) Orsakov C. Glucagon-like peptide-1, a new hormone of the enteroinsular axis. *Diabetologia* **1992**, *35*, 701–711. (c) Drucker, D. J. Glucagon-Like Peptides. *Diabetes* **1998**, *47*, 159–169.
- (5) (a) Mentlein, R.; Gallwitz, B.; Schmidt, W. E. Dipeptidyl-peptidase IV hydrolyzes gastric inhibitory polypeptide, glucagon-like peptide-1 (7–36), peptide histidine methionine and is responsible for their degradation in human serum. *Eur. J. Biochem.* **1993**, *214*, 829–835. (b) Deacon, C. F.; Johnsen, A. H.; Holst, J. J. Degradation of glucagon-like peptide-1 by human plasma in vitro yields an N-terminally truncated peptide that is a major endogenous metabolite in vivo. *J. Clin. Endocrinol. Metab.* **1995**, *80*, 952–957. (c) Kieffer, T. J.; McIntosh, C. H. S.; Pederson, R. A. Degradation of glucose-dependent insulinotropic polypeptide and truncated glucagon-like peptide-1 in vitro and in vivo by dipeptidyl peptidase IV. *Endocrinology* **1995**, *136*, 3585–3596. (d) Lene, H.; Deacon, C. F.; Orskov, C.; Holst, J. J. Glucagon-like peptide-1-(7–36) amide is transformed to glucagon-like peptide-1-(9–36) amide by dipeptidyl peptidase IV in the capillaries supplying the L cells of the porcine intestine. *Endocrinology* **1999**, *140*, 5356–5363.
- (6) Ahren, B.; Holst, J. J.; Martensson, H.; Balkan, B. Improved glucose tolerance and insulin secretion by inhibition of dipeptidyl peptidase IV. *Eur. J. Pharmacol.* **2000**, *404* (1/2), 239–245.
- (7) Deacon, C. F.; Hughes, T. E.; Holst, J. J. Dipeptidyl peptidase IV inhibition potentiates the insulinotropic effect of glucagon-like peptide 1 in the anesthetized pig. *Diabetes* **1998**, *47*, (5), 764–769.
- (8) (a) Pederson, R. P.; White, H. A.; Schlenzig, D.; Pauly, R. P.; McIntosh, C. R. P.; Demuth, H. U. Improved glucose tolerance in Zucker fatty rats by oral administration of the dipeptidyl peptidase IV inhibitor isoleucine thiazolidide. *Diabetes* **1998**, *47*, (8) 1253–1258. (b) Pauly, R. P.; Demuth, H.-U.; Rosche, R.; Schmidt, J.; White H. A.; Lynn F.; McIntosh, C. H. S.; Pederson, R. A. Improved glucose tolerance in rats treated with the dipeptidyl peptidase IV (CD26) inhibitor Ile-thiazolidide. *Metabolism* **1999**, *3*, 385–389. (c) Pospisilik, J. A.; Stafford, S. G.;

- Demuth, H.-U.; Brownsey, R.; Parkhouse, W.; Finegood, D. T.; McIntosh, C. H. S. Pederson, R. A. Long-Term Treatment with the Dipeptidyl Peptidase IV Inhibitor P32/98 causes sustained improvements in glucose tolerance, insulin sensitivity, hyperinsulinemia, and β -cell glucose responsiveness in VDF (fa/fa) Zucker Rats. *Diabetes* **2002**, *51*, 943–950.
- (9) (a) Balkan, B.; Kwasnik, L.; Miserendino, R.; Holst, J. J.; Li, X. Inhibition of dipeptidyl peptidase IV with NVP-DPP728 increases plasma GLP-1 (7–36 amide) concentrations and improves oral glucose tolerance in obese Zucker rats. *Diabetologia* **1999**, *42* (11), 1324–1331. (b) Mitani, H.; Takimoto, M.; Hughes T. E.; Kimur, M. Dipeptidyl peptidase IV inhibition improves impaired glucose tolerance in high-fat diet-fed rats: study using a Fisher 344 rat substrain deficient in its enzyme activity. *Japanese Journal of Pharmacology* **2002**, *88*, 442–450. (c) Mitani, H.; Takimoto, M. and Kimura, M. Dipeptidyl peptidase IV inhibitor, NVP-DPP728, ameliorates early insulin response and glucose tolerance in aged rats but not in aged Fisher 344 rats lacking its enzyme activity. *Jpn J. Pharmacol.* **2002**, *88*, 451–458.
- (10) Sudre, B.; Broqua, P.; White, R. B.; Ashworth, D.; Evans, E. M.; Haigh, R.; Junien, J.-L.; Aubert, M. L. Chronic Inhibition of Circulating Dipeptidyl Peptidase-IV by FE 999011 Delays the Occurrence of Diabetes in Male Zucker Diabetic Fatty Rats. *Diabetes* **2002**, *51*, 1461–1469.
- (11) Marguet, D.; Baggio, L.; Kobayashi, T.; Bernard, A.-M.; Pierres, M.; Nielsen, P. F.; Ribel, U.; Wantanabe, T.; Drucker, D. J.; Wagtmann, N. Enhanced insulin secretion and improved glucose tolerance in mice lacking CD26. *Proc. Natl. Acad. Sci. U.S.A.* **2000**, *97*, 6864–6879.
- (12) Holst, J. J.; Deacon, C. F. Inhibition of the activity of Dipeptidyl-Peptidase IV as a treatment for Type 2 Diabetes. *Diabetes* **1998**, *47*, 1663–1670. (b) Zander, M.; Madsbad, S.; Madsen, J. L.; Holst, J. J. Effect of 6-week course of glucagon-like peptide 1 on glycaemic control, insulin sensitivity, and β -cell function in type 2 diabetes; a parallel-group study. *Lancet* **2002**, *359*, 824–830.
- (13) (a) Ahren, B.; Larsson, J.; Holst, J. J. Effects of glucagon-like peptide-1 on islet function and insulin sensitivity in noninsulin dependent diabetes mellitus. *J. Clin. Endocrinol. Metab.* **1997**, *82*, 473–478. (b) Rachman, J.; Borrow, B. A.; Levy, J. C.; Turner R. C. Near normalization of diurnal glucose concentrations by continuous administration of glucagon-like peptide 1 (GLP-1) in subjects with NIDDM. *Diabetologia* **1997**, *40*, 205–211. (c) Nauck, M. A.; Wollschlaeger, D.; Werner, J.; Holst, J. J.; Orskov, C.; Creutzfeldt, W.; Willms, B. Effects of subcutaneous glucagon-like peptide 1 (GLP-1 [7–36 amide]) in patients with NIDDM. *Diabetologia* **1996**, *39*, 1546–1553. (d) Drucker, D. J. Biological actions and therapeutic potential of the glucagon-like peptides. *Gastroenterology* **2002**, *122* (2), 531–544. (e) Egan, J.; Cloquet, A. R.; Elahi, D. The Insulinotropic Effect of Acute Exendin-4-administered to Humans: Comparison of Nondiabetic State to Type 2 Diabetes. *J. Clin. Endocrinol. Metab.* **2002**, *87* (3), 1282–1290.
- (14) (a) Wettergren, A.; Schjoldager, B.; Martensen, P. E.; Myhre, J.; Christiansen, J.; Holst, J. J. Truncated GLP-1 (proglucagon 72–107 amide) inhibits gastric and pancreatic functions in man. *Dig. Dis. Sci.* **1993**, *38*, 665–673. (b) Nauck, M. A.; Niedereichholz, U.; Ettl, R.; Holst, J. J.; Orskov, C.; Ritzel, R.; Schmiegel, W. H. Glucagon-like peptide-1 inhibition of gastric-emptying outweighs its insulinotropic effects in healthy humans. *Am. J. Physiol.* **1997**, *273*, E981–E988. (c) Nauck, M. A. Is GLP-1 an incretin hormone? *Diabetologia* **1999**, *42*, 373–379. (d) Egan, J.; Cloquet, A. R.; Elahi, D. The Insulinotropic Effect of Acute Exendin-4-Administered to Humans: Comparison of Nondiabetic State to Type 2 Diabetes. *J. Clin. Endocrinol. Metab.* **2002**, *87* (3), 1282–1290.
- (15) (a) Habener, J. F. Glucagonlike peptide-1 agonist stimulation of β -cell growth and differentiation. *Curr. Opin. Endocrinol. Diabetes* **2001**, *8* (2), 74–81. (b) Ling, Z.; Wu, D.; Zambre, Y.; Flamez, D.; Drucker, D. J.; Pipeleers, D. G.; Schuit, F. C. Glucagon-like peptide 1 receptor signaling influences topography of islet cells in mice. *Virchows Arch.* **2001**, *438* (4), 382–387. (c) Aspelun, F.; Egan, J. M.; Slezak, L. A.; Sritharan, K. C.; Elahi, D.; Andersen, D. K. Glucagon-like peptide-1 and exendin-4 improve glucose tolerance and induce islet cell growth in pancreatitis in rats. *Surg. Forum* **2000**, *51*, 40–42. (d) Kemp, D. M.; Habener, J. F. Insulinotropic hormone glucagon-like peptide 1 (GLP-1) activation of insulin gene promoter inhibited by p38 mitogen-activated protein kinase. *Endocrinology* **2001**, *142* (3), 1179–1187. (e) Parkes, D. G.; Pittner, R.; Jodka, C.; Smith, P.; Young, A. Insulinotropic actions of exendin-4 and glucagon-like peptide-1 in vivo and in vitro. *Metab. Clin. Exp.* **2001**, *50* (5), 583–589. (f) Farilla, L.; Hui, H.; Berolotto, C.; Kang, E.; Bulotta, A.; Di Mario, U.; Perfetti, R. Glucagon-like Peptide-1 promotes islet cell growth and inhibits apoptosis in Zucker diabetic rats. *Endocrinology* **2002**, *143* (11), 4397–4408. (g) Abraham, E. J.; Leech, C. A.; Lin, J. C.; Zuelwski, H.; Habener, J. F. Insulinotropic Hormone Glucagon-Like Peptide-1 differentiation of Human Pancreatic Islet-Derived Progenitor Cells into Insulin-Producing Cells. *Endocrinology* **2002**, *143* (8), 3152–3161. (h) Turrel, C.; Bailbe, D.; Lacorne, M.; Meile, M. J.; Kergoat, M.; Portha, B. Persistent Improvement of Type 2 Diabetes in the Goto-Kakizaki Rat Model by Expansion of the B-Cell Mass During the Prediabetic Period with Glucagon-Like Peptide-1 or Exendin-4. *Diabetes* **2002**, *51*, 1443–1452. (i) Perfetti, R.; Zhou, J.; Doyle, M. E.; Egan, J. M. Glucagon-Like Peptide –1 Induces Cell Proliferation and Pancreatic-Duodenum Homeobox-1 Expression and Increases Endocrine Cell Mass in the Pancreas of Old, Glucose-Intolerant Rats. *Endocrinology* **2000**, *141* (12), 4600–4605. (j) Li, Y.; Hansotia, T.; Yusta, B.; Ris, F.; Halban, P. A.; Drucker, D. J. Glucagon-like Peptide-1 Receptor Signaling Modulates beta Cell Apoptosis. *J. Biol. Chem.* **2003**, *278* (1), 471–478.
- (16) (a) Flint, A.; Raben, A.; Ersboll, A. K.; Holst, J. J.; Astrup, A. The effect of physiological levels of glucagon-like peptide-1 on appetite, gastric emptying, energy and substrate metabolism in obesity. *Int. J. Obes.* **2001**, *25*, 781–792.
- (17) (a) Doyle, M. E.; Egan, J. M. Glucagon-like peptide-1. *Recent Prog. Horm. Res.* **2001**, *56*, 377–399. (b) Villanueva-Peñacarrillo, M. L.; Puente, J.; Redondo, A.; Clemente, F.; Valverde, I. Effect of GLP-1 treatment on GLUT2 and GLUT4 expression in Type 1 and Type 2 rat diabetic models. *Endocrine* **2001**, *15* (2), 241–248. (c) Sandhu, H.; Wiesenthal, S. R.; MacDonald, P. E.; McCall, R. H.; Tchipashvili, V.; Rashid, S.; Satkunarajah, M.; Irwin, D. M.; Shi, Z. Q.; Brubaker, P. L.; Wheeler, M. B.; Vranic, M.; Efendic, S.; and Giacca, A. Glucagon-Like Peptide 1 increases insulin sensitivity in depancreatized dogs. *Diabetes* **1999**, *48*, 1045–1053. (d) Pospisilik, J. A.; Stafford, S. G.; Demuth, H.-U.; McIntosh, H. S.; Pederson, R. A. Long-Term Treatment with Dipeptidyl Peptidase IV Inhibitor Improves Hepatic and Peripheral Insulin Sensitivity in the VDF Zucker Rat – A Euglycemic-Hyperinsulinemic Clamp Study. *Diabetes* **2002**, *51*, 2677–2683.
- (18) (a) Burcelin, R.; Da Costa, A.; Drucker, D.; Thorens, B. Glucose competence of the hepatoprotal vein sensor requires the presence of an activated glucagon-like peptide-1 receptor. *Diabetes* **2001**, *50*, 1720–1728. (b) Balkan, B.; Li, X. Portal GLP-1 administration in rats augments the insulin response to glucose via neuronal mechanisms. *Am. J. Physiol. Regul. Integr. Comput. Physiol.* **2000**, *279*: R1449–R1454.
- (19) (a) Juana, F.; Valdeolillos, M. Glucose-dependent stimulatory effect of glucagon-like peptide 1(7–36) amide on the electrical activity of pancreatic β -cells recorded in vivo. *Diabetes* **1999**, *48* (4), 754–757. (b) Nauck, M. A.; Heimesat, M. M.; Behle, K.; Holst, J. J.; Nauck, M. S.; Ritzel, R.; Hufner, M.; Schmiegel, Wolff, H. Effects of glucagon-like peptide 1 on counterregulatory hormone responses, cognitive functions, and insulin secretion during hyperinsulinemic, stepped hypoglycemic clamp experiments in healthy volunteers. *J. Clin. Endocrinol. Metab.* **2002**, *87* (3), 1239–1246.
- (20) These nonsubstrate DPP-IV inhibitors provide low micromolar IC50's, and, except for refs 20(a) and 20(b), contain a protonatable amine: (a) Shimazawa, R.; Takayama, H.; Kato, F.; Kato, M.; Hashimoto, Y. Nonpeptide small-molecular inhibitors of Dipeptidyl Peptidase IV; N-phenylphthalimide analogues. *Bioorg. Med. Chem. Lett.* **1999**, *9*, 559–562. (b) Miyachi, H.; Kato, M.; Kato, F.; Hashimoto, Y. Novel potent nonpeptide aminopeptidase N inhibitors with a cyclic imide skeleton. *J. Med. Chem.* **1998**, *41*, 3, 263–265. (c) Yamada, M.; Okagaki, C.; Higashijima, T.; Tanaka, S.; Ohnuki, T.; Sugita, T. A potent dipeptide inhibitor of dipeptidyl peptidase IV. *Bioorg. Med. Chem. Lett.* **1998**, *8*, 1537–1540. (d) Coppola, G. M.; Zhang, Y. L.; Schuster, H. F.; Russell, M. E.; Hughes T. E. 1-Aminomethylisoquinoline-4-carboxylates as novel Dipeptidyl Peptidase IV inhibitors. *Bioorg. Med. Chem. Lett.* **2000**, *10*, 1555–1558. (e) Kanstrup, A. B.; Christiansen, L. B.; Lundbeck, J. M.; Kristiansen, M. Preparation of piperazinylpurinediones as inhibitors of dipeptidylpeptidase IV. Patent WO 02002560, July 4th, 2002.
- (21) Irreversible oligopeptides with the N-terminal X-Pro-X sequence (low micromolar IC50) – Rahfeld, J.; Schierhorn, M.; Hartrodt, B.; Neubert, K.; Heins, J. Are Diprotin A and (Ile-Pro-Ile) and Diprotin B (Val-Pro-Leu) Inhibitors or Substrates of Dipeptidyl Peptidase IV? *Biochim. Biophys. Acta* **1991**, *1076*, 314–316.
- (22) Suicide substrate (latent quinoniminium methide electrophile – large cyclopeptide). Nguyen, C.; Blanco, J.; Mazaleyra, J. P.; Krust, B.; Callebaut, C.; Jacotot, E.; Hovanessian, A. G.; Wakselman, M. Specific and Irreversible Cyclopeptide Inhibitors of Dipeptidyl Peptidase IV Activity of the T-Cell Activation Antigen CD26. *J. Med. Chem.* **1998**, *41*, 2100–2110.
- (23) Heins, J.; Welker, P.; Schönlein, C.; Born, I.; Hartrodt, B.; Neubert, K.; Tsuru, D.; Barth, A. Mechanism of Proline-Specific Proteinases; (I) Substrate Specificity of Dipeptidyl Peptidase IV from Pig Kidney and Protein-Specific Endopeptidase from *Flavobacterium meningosepticum*. *Biochim. Biophys. Acta* **1988**, *954*, 161–169.

- (24) (a) Barth, A.; Heins, J.; Fischer, G.; Neubert, K.; Schneeweiss, B. Dipeptidyl-peptidase IV: mechanism and specificity of the substrate cleavage. *Mol. Cell. Regul. Enzyme Act., Part 1-3* **1984**, *46*, 297–339. (b) Schön, E.; Born, I.; Demuth, H.-U.; Faust, J.; Neubert, K.; Steinmetzer, T.; Barth, A.; Ansorge, S. Dipeptidyl Peptidase IV in the Immune System., *Biol. Chem. Hoppe-Seyler* **1991**, *372*, 305–311.
- (25) For comprehensive reviews on DPP-IV inhibitors, please see the following. (a) Villhauer, E. B.; Coppola, G. M.; Hughes, T. E. DPP-IV inhibition and Therapeutic Potential. *Annu. Rep. Med. Chem.* **2001**, *36*, 191–200. (b) Augustyns, K.; Bal, G.; Thonus, G.; Belyaev, A.; Zhang, X. M.; Bollaert, W.; Lambeir, A. M.; Durinx, C.; Goossens, F.; Haemers A. The Unique Properties of Dipeptidyl-Peptidase IV (DPP-IV/CD26) and the Therapeutic Potential of DPP-IV Inhibitors *Curr. Med. Chem.* **1999**, *6*, 311–327. (c) Snow, R. J.; Bachovchin, W. W. Boronic acid inhibitors of dipeptidyl peptidase IV; a new class of immunosuppressive agents. *Adv. Med. Chem.* **1995**, *3*, 149–177.
- (26) Jenkins, P. D.; Jones, D. M. DP-IV-serine protease inhibitors, Patent WO 95/15309, June 8th, 1995.
- (27) Ashworth, D. M.; Atrash, B.; Baker, G. R.; Baxter, A. J.; Jenkins, P. D. 2-Cyanopyrrolidides as potent, stable inhibitors of Dipeptidyl Peptidase IV. *Bioorg. Med. Chem. Lett.* **1996**, *6*, (10), 1163–1166.
- (28) Li, J.; Wilk, E.; Wilk, S. Aminoacylpyrrolidine-2-nitriles: Potent and stable inhibitors of Dipeptidyl-Peptidase IV (CD26). *Arch. Biochem. Biophys.* **1995**, *323* (1), 148–154.
- (29) Ashworth, D. M.; Atrash, B.; Baker, G. R.; Baxter, A. J.; Jenkins, P. D. 4-Cyanothiazolidides as very potent, stable inhibitors of Dipeptidyl Peptidase IV. *Bioorg. Med. Chem. Lett.* **1996**, *6*, (22), 2745–2748.
- (30) Villhauer, E. B.; Brinkman, J. A.; Naderi, G. B.; Dunning, B. E.; Mangold, B. L.; Mone M. D.; Russell M. E.; Weldon, S. C.; Hughes T. E. 1-[2-[(5-Cyanopyridin-2-yl)amino]ethylamino]-acetyl-2-(S)-pyrrolidine-carbonitrile: a Potent, Selective and Orally Bioavailable Dipeptidyl Peptidase IV Inhibitor with Antihyperglycemic Properties, *J. Med. Chem.* **2002**, *45*, 2362–2368.
- (31) Villhauer, E. B. N-(Substituted glycly)-2-cyanopyrrolidides, Pharmaceutical compositions containing them and their use in inhibiting Dipeptidyl Peptidase-IV. US 6,011,155, January 4th, 2000.
- (32) Villhauer, E. B. N-(Substituted glycly)-2-cyanopyrrolidides, Pharmaceutical compositions containing them and their use in inhibiting Dipeptidyl Peptidase-IV. US 6,166,063, December 26th, 2000.
- (33) Villhauer, E. B. N-(Substituted glycly)-2-cyanopyrrolidides, Pharmaceutical compositions containing them and their use in inhibiting Dipeptidyl Peptidase-IV. US 6,432,969, August 13th, 2002.
- (34) ORTEP drawings and atomic coordinate information of NVP-DPP728 (**8c**) and NVP-LAF237 (**12j**) atomic coordinate information can be obtained from Supporting Information of ref 30 and this paper, respectively.
- (35) Described in Experimental Section.
- (36) Hughes, T. E.; Mone, M. D.; Russell, M. E.; Weldon, S. C.; Villhauer, E. B. NVP-DPP728 (1-[[[2-[(5-cyanopyridin-2-yl)-amino]ethyl]amino]acetyl]-2-cyano-(S)-pyrrolidine), a slow-binding inhibitor of Dipeptidyl Peptidase IV. *Biochemistry* **1999**, *38*, 11597–11603.
- (37) Augustyns, K. J. L.; Lambeir, A. M.; Borloo, M.; De Meester, I.; Vedernikova, I.; Vanhoof, G.; Handriks, D.; Scharpe, S.; Haemaers, A. Pyrrolidides; synthesis and structure–activity relationship as inhibitors of dipeptidyl peptidase IV. *Eur. J. Med. Chem.* **1997**, *32*, 301–309.
- (38) PPCE and DPP-II are the standard enzymes in DPP-IV selectivity studies. (a) Belyaev, A.; Zhang, X.; Augustyns, K.; Lambeir, A. M.; De Meester, I.; Verdernikova, I.; Scharpe, S.; Haemers, A. Structure–Activity Relationship of Diaryl Phosphonate Esters a Potent Irreversible Dipeptidyl Peptidase IV Inhibitors. *J. Med. Chem.* **1999**, *42*, 1041–1052. (b) Sedo, A.; Malik, R. Dipeptidyl peptidase IV-like molecules: homologous proteins or homologous activities. *Biochim. Biophys. Acta* **2001**, *1550*, 107–116.
- (39) Rasmussen, H. P.; Branner, S.; Wiberg, F. C.; Wagtmann, N. Crystal structure of human dipeptidyl peptidase IV/CD26 in complex with a substrate analogue. *Nature Struct. Biol.* **2003**, *10* (1), 19–25.
- (40) (a) Rothenberg, P.; Kalbag, J.; Smith, H. T.; Gingerich, R.; Nedelman, J.; Villhauer, E.; McLeod, J.; Hughes, T. Treatment with a DPP-IV Inhibitor, NVP-DPP728, Increases Prandial Intact GLP-1 Levels and Reduces Glucose Exposure in Humans. *Diabetes* **2000**, *49*, (1), A39. (b) Ahrén, B.; Simonsson, E.; Larsson, H.; Landin-Olsson, M.; Torgeirsson, H.; Jansson, P. A.; Sandqvist, M.; Båvenholm, P.; Efendic, S.; Eriksson, J. W.; Dickinson, S.; Holmes, D. Inhibition of Dipeptidyl Peptidase IV improves metabolic control over a 4 week study period in type 2 diabetes. *Diabetes Care* **2002**, *25* (5), 869–875.
- (41) Reimer, M. K.; Holst, J. J.; Ahrén, B. Long-term inhibition of dipeptidyl peptidase IV improves glucose tolerance and preserves islet function in mice. *Eur. J. Endocrinol.* **2002**, *146*, 717–727.
- (42) Reisher, S. R.; Hughes, T. E.; Ordovas, J. M.; Schaefer, E. J.; Feinstein, S. I. Increased expression of apolipoprotein genes accompanies differentiation in the intestinal cell line Caco-2. *Proc. Natl. Acad. Sci. U.S.A.* **1993**, *90*, 5757–5761.
- (43) Kubota, T.; Flentke, G. R.; Bachovchin, W. W.; Stollar, B. D. Involvement of dipeptidyl peptidase IV in an in vivo immune response. *Clin. Exp. Immunol.* **1992**, *89*, 192–197.
- (44) Macnair, R. D.; Kenny, A. J. Proteins of the Kidney Microvillar Membrane: The amphipathic Form of Dipeptidyl Peptidase IV. *Biochem. J.* **1979**, *179*, 379–395.
- (45) Mantle, D. Characterization of dipeptidyl and tripeptidyl aminopeptidases in human kidney soluble fraction. *Clin. Chim. Acta* **1991**, *196*, 135–142.
- (46) DeMeester, I.; Vanhoof, G.; Lambeir, A. M.; Scharpe, S. Use of immobilized adenosine deaminase for the rapid purification of native human CD26/dipeptidyl peptidase IV. *J. Immunol. Methods* **1996**, *189*, 99–105.
- (47) Nagatsu, T.; Sakai, T.; Kojima, K.; Araki, E.; Sakakibara, S.; Fukasawa, K.; Harada, M. A sensitive and specific assay for dipeptidyl-aminopeptidase II in serum and tissues by liquid chromatography-fluorometry. *Anal. Biochem.* **1985**, *147*, 80–85.
- (48) Momand, J.; Clarke, S. Rapid degradation of D- and L-succinimide-containing peptides by a post-proline endopeptidase from human erythrocytes. *Biochemistry* **1987**, *26*, 7798–7805.
- (49) Deacon, C. F.; Hughes, T. E.; Holst, J. J. Dipeptidyl peptidase IV inhibition potentiates the insulinotropic effect of glucagon-like peptide 1 in the anesthetized pig. *Diabetes* **1998**, *47*, (5), 764–769.

JM030091L